



# Empirical glacier mass-balance models for South America

Sebastian G. Mutz  and Johannes Aschauer\*

Department of Geosciences, University of Tübingen, Germany

## Article

\*Now at the WSL Institute for Snow and Avalanche Research SLF, Switzerland

**Cite this article:** Mutz SG, Aschauer J (2022). Empirical glacier mass-balance models for South America. *Journal of Glaciology* **68**(271), 912–926. <https://doi.org/10.1017/jog.2022.6>

Received: 29 June 2021

Revised: 19 January 2022

Accepted: 20 January 2022

First published online: 18 February 2022

### Keywords:

Climate change; glacier mass-balance; glacier modelling; mountain glaciers

### Author for correspondence:

Sebastian Mutz,

E-mail: [sebastian.mutz@uni-tuebingen.de](mailto:sebastian.mutz@uni-tuebingen.de)

## Abstract

We investigate relationships between synoptic-scale atmospheric variability and the mass-balance of 13 Andean glaciers (located 16–55° S) using Pearson correlation coefficients (PCCs) and multiple regressions. We then train empirical glacier mass-balance models (EGMs) in a cross-validated multiple regression procedure for each glacier. We find four distinct glaciological zones with regard to their climatic controls: (1) The mass-balance of the Outer Tropics glaciers is linked to temperature and the El Niño-Southern Oscillation ( $PCC \leq 0.6$ ), (2) glaciers of the Desert Andes are mainly controlled by zonal wind intensity ( $PCC \leq 0.9$ ) and the Antarctic Oscillation ( $PCC \leq 0.6$ ), (3) the mass-balance of the Central Andes glaciers is primarily correlated with precipitation anomalies ( $PCC \leq 0.8$ ), and (4) the glacier of the Fuegian Andes is controlled by winter precipitation ( $PCC \approx 0.7$ ) and summer temperature ( $PCC \approx -0.9$ ). Mass-balance data in the Lakes District and Patagonian Andes zones, where most glaciers are located, are too sparse for a robust detection of synoptic-scale climatic controls. The EGMs yield  $R^2$  values of  $\sim 0.45$  on average and  $\leq 0.74$  for the glaciers of the Desert Andes. The EGMs presented here do not consider glacier dynamics or geometry and are therefore only suitable for short-term predictions.

## 1. Introduction

A large fraction of southern hemisphere glaciers is located in the Andes of South America (Pfeffer and others, 2014). Due to the Andes' high latitudinal and altitudinal range, its glaciers are situated in very different climatic conditions (Sagredo and Lowell, 2012). The northern section of the mountain range is subjected to a tropical climate, the subtropics of South America are hosting one of the driest regions on Earth, and the mid latitudes are humid and dominated by frontal systems (Fig. 1; Garreaud and others, 2009). Consequently, the Andes cover a broad range of glaciological regimes, and glaciers react differently to climatic disturbances (Sagredo and others, 2014, 2017).

South American glaciers follow the recent general trend of glacial retreat that is monitored worldwide (WGMS, 2017). Environmental and socioeconomic consequences of this development are manifold. Although mountain glaciers only hold  $\sim 0.12\%$  of the global freshwater resources, they play an important role in the global water cycle and regional water management (Shiklomanov, 1993). In regions such as the Dry Andes, where precipitation is concentrated in winter months, glaciers act as a freshwater reservoir in dry seasons (e.g. Kaser and others, 2003; Favier and others, 2009; Kaser and others, 2010; Burger and others, 2019). With a changing climate and accompanying ice mass loss in the Andes, this runoff smoothing effect is diminished and the point of maximum runoff has possibly been passed already (Ragettli and others, 2016; Huss and Hock, 2018). Furthermore, hydroelectric power supply, agricultural irrigation, water for human consumption and industrial processes can no longer be guaranteed in some areas in the future in case of the disappearance of Andean glaciers (Vergara and others, 2007). The receding of Patagonian glaciers may additionally lead to a decrease in local tourism and economy due to their value as tourist attractions (Vergara and others, 2007). Case studies of the Cotacachi glacier in Ecuador demonstrate how the disappearance of a glacier already results in a decline in agriculture, tourism and biodiversity in surrounding areas (Rhoades and others 2006; Vergara and others, 2007). About half of the global human population lives in coastal areas, making sea level rise one of the potentially most severe consequences of contemporary climate change (Leatherman, 2001; Douglas and others, 2001). Although mountain glaciers make up only a relatively small fraction of stored solid water on Earth compared to the ice sheets of Greenland and Antarctica, mountain glaciers are estimated to contribute 25–30% to the observed sea level rise in the period 1961–2016 due to faster reactions to the changing climate (Meier, 1984; Kaser and others, 2006; Zemp and others, 2019; IPCC, 2021). The total water stored in the glaciers of the Southern Andes represents a mean sea level equivalent of  $\sim 13$  mm (Stocker and others, 2013; Farinotti and others, 2019) and ice volume of  $\sim 5.34 \pm 1.39 \cdot 10^3$  km<sup>3</sup> (Farinotti and others, 2019).

The above described observed and potential consequences of glacial retreat stress the need for accurate model-based predictions of mountain glacier mass-balance changes to allow for more informed mitigation strategies and policy making. Additionally, glacier modelling can provide insights into past climate conditions and complement palaeoclimate modelling and dating of past glacial geometries (Hostetler and Clark, 2000; Hulton and others, 2002; Kull and others, 2003). Finally, model-based estimates of the evolution of mountain glaciers in the geologic past can provide insight into their erosional capacity and potential impact on

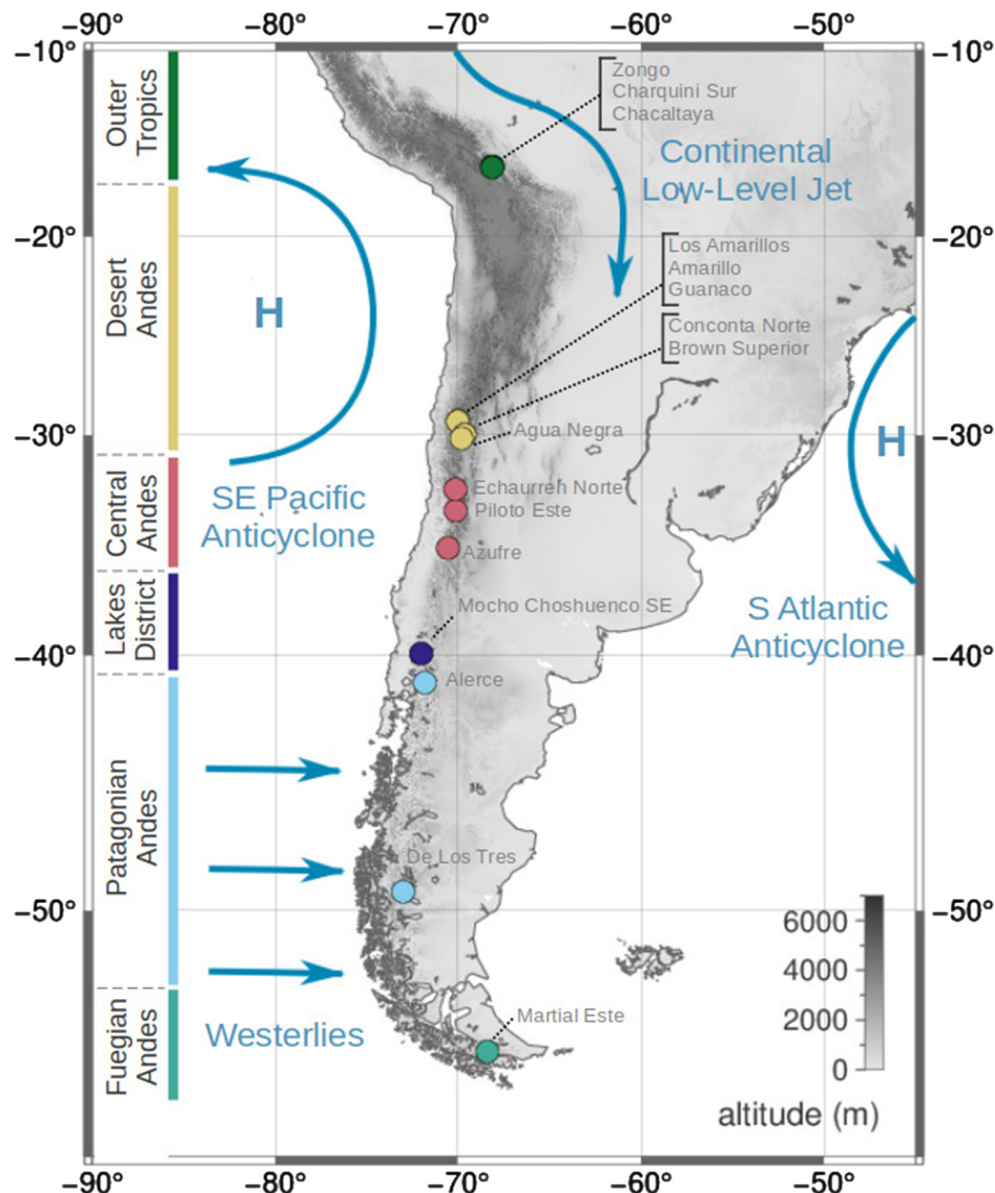


**Fig. 1.** Overview of South American climatic conditions (dark blue) and the locations (circles) and geographic classifications (circle colours) of the glaciers in this study. The glaciers are categorised with respect to prevailing regional geographic conditions. These categories are largely based on the glaciological zones proposed and used by Lliboutry (1998), updated by Barcaza and others (2017), and Zalazar and others (2020).

mountain building processes (Egholm and others, 2009; Thomson and others, 2010) and thus complement ongoing research of the interactions between tectonics, climate and Earth surface processes in mountain regions (e.g. Mutz and Ehlers, 2019).

Several approaches to model glacier mass-balance have been applied to glaciers in South America. These include techniques from the super-categories of empirical and physical (process-based) models. The spatial coverage of studies ranges from single glaciers to continental scale assessments of glacier changes (Fernández and Mark, 2016). Dynamical, numerical mass-balance models describe and parameterise physical processes on a glacier. Atmospheric variables, such as precipitation and temperature, are used as boundary conditions. These models are commonly classified by their implementation of ablation processes: Degree day models estimate the surface mass loss on a glacier on a daily basis using temperature (e.g. Tangborn, 1999), while energy-balance models capture ablation processes based on radiation, longwave fluxes, sensible and latent heat (e.g. Oerlemans, 1992). More sophisticated models calculate the energy budget on a

glacier by including parameters such as humidity, pressure, snow-drift, snowpack evolution and runoff processes in addition to temperature and precipitation (Oerlemans, 1993; Mernild and others, 2017). These models typically have tuning parameters that need to be derived empirically with measurements of mass-balance and climate elements. Therefore, the above described models rely on fine-scaled atmospheric data in the vicinity of the glacier. When coupling these glacier models to the relatively coarse output of general circulation models (GCMs), climate simulations have to be downscaled first to fit the needs of the mass-balance model (e.g. Reichert and others, 2001; Schaefer and others, 2013; Mernild and others, 2017). The two main downscaling approaches are numerical and empirical-statistical downscaling (ESD) (for a review on downscaling strategies, see Giorgi and others, 2001). Numerical downscaling uses an approximation for underlying physical processes in order to make predictions of regional weather conditions based on a larger-scale atmospheric state. ESD uses empirical-statistical relationships of local-scale meteorological measurements and large-scale climate patterns (Wilby and others, 2004). ESD-based modelling assumes the temporal stationarity of

these relationships. When driving glacier models with downscaled climate conditions, uncertainties introduced in the downscaling process are potentially propagated in the modelling of glacier mass-balance and add another layer of uncertainty to the uncertainties of capturing complex physical processes of a glacier.

Alternatively, one can employ statistical techniques (e.g. Hoinkes, 1968; Lliboutry, 1974; Condom and others, 2007) or apply a modification of the ESD approach directly on the glaciers to estimate changes in their mass-balance (e.g. Schöner and Böhm, 2007; Mutz and others, 2015). In such a procedure, glacier mass-balance replaces local atmospheric variables as the prediction target (predictand), thus circumventing the costly intermediate step of climate downscaling. Since local geographic conditions are implicitly included in empirical models, it also removes the need to explicitly parameterise those for the location of the investigated glaciers. This approach requires sufficiently long and temporally overlapping measurements of atmospheric predictors and glacier mass-balance in order to adequately capture robust empirical transfer functions between them. Furthermore, it requires knowledge of glacier-climate interactions in the region to ensure that physically meaningful predictors are chosen and captured. Empirical relationships represent underlying physical processes. The growing South American mass-balance record lends itself to this approach, and previous studies of relationships between atmospheric quantities and South American glaciers (Sagredo and Lowell, 2012; Mernild and others, 2015; Maussion and others, 2015; Veettil and others, 2016) allow for a well-informed selection of predictors. While some studies have used an empirical approach on a small selection of glaciers in South America (Manciati and others, 2014; Maussion and others, 2015), none have taken full advantage of available mass-balance records to assess mass-balance changes in context of synoptic-scale climate and generate future estimates across South America.

In this study, an ESD approach is applied to a selection of Andean glaciers south of 15°S. ESD-based empirical glacier mass-balance models (EGMs) are trained for individual glaciers. They capture the transfer functions between glacier mass-balance variations and large-scale climate variability obtained from ERA-Interim reanalysis. In order to demonstrate the application of such models, the EGMs are then coupled to simulations of the Max-Planck-Institute's Earth System Model (MPI-ESM-MR) of the Coupled Model Intercomparison Project (CMIP5) to estimate the mass-balance response to potential future climate change under different greenhouse gas (GHG) concentration scenarios (see Supplementary material). The following goals are addressed by this study:

- To identify synoptic-scale atmospheric predictors of South American glacier mass-balance and quantify their influence.
- To assess the potential of an ESD-based modelling approach for South American glacier mass-balance.
- To generate, evaluate and apply EGMs for each Andean glacier that is suitable for an ESD-based modelling approach.

## 2. Data and methods

### 2.1 Glaciers in South America

The response of glacier front variations to external forcing depends on topography and glacier size, and can result in time lags of up to several years (Müller, 1987; Jóhannesson and others, 1989; Cuffey and Paterson, 2010). Therefore, glacier extent and frontal variation are not well suited for statistical mass-balance models (Hodge and others, 1998) and the models in this study are trained with glacier-wide mass-balances based on observational records constructed with the glaciologic method described

in Braithwaite (2002). These data are provided by the World Glacier Monitoring Service (WGMS) database (WGMS, 2018). Due to the requirements of the ESD approach, our first selection of glaciers restricted to those with annual mass-balance ( $B_a$ ) records covering at least 10 years in succession. Eleven South American glaciers fulfill these requirements. They are located in a latitudinal range of 16°S to 55°S and different climatic and glaciological zones (Fig. 1, Lliboutry (1998), updated by Barcaza and others (2017), and Zalazar and others (2020)). Five additional glaciers, Agua Negra (AGN), Azufre (AZF), Alerce (ALC), Mocho Choshuenco SE (MCH) and De Los Tres (DLT), are included in our study to increase the number of representatives for South American glaciological zones. Our study thus considers glaciers of the Outer Tropics (Zongo (ZON), Charquini Sur (CHS), Chacaltaya (CHT)), Desert Andes (Los Amarillos (LAM), Amarillo (AMA), Guanaco (GUA), Conconta Norte (CON), Brown Superior (BRO) and AGN), Central Andes (Echaurren Norte (ECH)), Piloto Este (PIL and AZF), Lakes District (MCH), Patagonian Andes (ALC and DLT) and Fuegian Andes (Martial Este (MAR)). The mass-balance records for MCH and DLT are sufficiently long to include them in our analyses computationally despite not meeting the procedures' requirements listed above. Glacier names, acronyms, geographical setting and record length are summarised in Table 1. Overviews of annual and seasonal mass-balance changes and recent cumulative mass loss are provided in Figures 2 and 3 respectively. Mass-balance data are given in units of meters water equivalent (m w.e.), i.e. the mass change per unit area divided by the density of water (Cogley and others, 2011).

### 2.2 ERA-Interim reanalysis

ERA-Interim reanalysis data of the European Centre for Medium-Range Weather Forecast (ECMWF) (Berrisford and others, 2011) is a global, homogenous dataset compiled with a data assimilation scheme which combines local observations of the atmospheric state with a dynamical numerical model. This scheme allows interpolations of observations in a physically consistent way (Dee and others, 2011). The dataset covers the period from 1979 onward and is updated regularly in real time (Berrisford and others, 2011). Data assimilation is done in 60 vertical model levels from the land surface up to the 0.1 hPa pressure level (Dee and others, 2011). The model output of the reanalysis is interpolated onto a 0.75° × 0.75° native longitude-latitude grid. At the equator, this roughly represents a 80 km × 80 km grid spacing (Dee and others, 2011). Monthly averages of daily mean values of the ERA-Interim dataset are used to calculate predictors for the mass-balance modelling (see Predictor construction section).

### 2.3 Empirical-statistical glacier mass-balance models

#### 2.3.1 Predictor construction

Potential predictors for empirical mass-balance modelling are chosen on the basis of their physical relevance to glacier mass-balance changes. More specifically, the criteria for consideration is the predictors known ability to alter surface energy balance, accumulation or other processes that influence the mass-balance of mountain glaciers. Additionally, the predictors should be adequately represented in GCMs to merit the EGM-GCM coupling.

Local precipitation and temperature are the main direct controls for accumulation and ablation respectively (Oerlemans and Reichert, 2000; Sagredo and others, 2014). We therefore use synoptic-scale atmospheric variables that are known to be good predictors for regional temperature and precipitation (Huth, 2002; Cavazos and Hewitson, 2005; Garreaud and others, 2013;

**Table 1.** Names, acronyms, geographical position, elevation range, area, setting and number of available mass-balance measurements (annual mass-balance ( $B_a$ ), winter mass-balance ( $B_w$ ) and summer mass-balance ( $B_s$ )) for each glacier used in this study (until mid-2019)

Name	Acronym	Lat [°N]	Lon [°E]	Elevation (m)	Area (km <sup>2</sup> )	Zone	No. of Records		
							$B_a$	$B_w$	$B_s$
Zongo	ZON	−16.280	−68.140	4939–6109	1.9 (2015)	Outer Tropics	24	0	0
Charquini Sur	CHS	−16.303	−68.107	5000–5334	0.3 (2015)	Outer Tropics	13	0	0
Chacaltaya	CHT	−16.351	−68.127	5230–5330	0 (2008)	Outer Tropics	17	5	5
Los Amarillos	LAM	−29.296	−69.995	4915–5535	0.8 (2015)	Desert Andes	10	2	2
Amarillo	AMA	−29.303	−70.001	5160–5315	0.2 (2015)	Desert Andes	10	2	2
Guanaco	GUA	−29.348	−70.016	5007–5356	1.6 (2015)	Desert Andes	12	4	4
Conconta Norte	CON	−29.976	−69.645	4950–5125	0.1 (2015)	Desert Andes	10	6	6
Brown Superior	BRO	−29.983	−69.642	4965–5115	0.2 (2015)	Desert Andes	10	6	6
Agua Negra	AGN	−30.165	−69.809	4750–5208	1.0 (2021)	Desert Andes	4	4	4
Piloto Este	PIL	−32.589	−70.142	4285–4715	0.6 (2013)	Central Andes	24	24	24
Echaurren Norte	ECH	−33.578	−70.131	3650–3880	0.4 (2000)	Central Andes	42	42	42
Azufre	AZF	−35.290	−70.550	3067–3978	2.3 (2021)	Central Andes	1	1	1
Mocho Choshuenco SE	MCH	−39.945	−72.015	1600–2422	5.0 (2019)	Lakes District	9	1	1
Alerce	ALC	−41.170	−71.820	1460–1975	2.3 (2012)	Patagonian Andes	0	0	0
De Los Tres	DLT	−49.330	−73.000	1200–1990	1.0 (1998)	Patagonian Andes	8	7	7
Martial Este	MAR	−54.780	−68.400	940–1170	0.1 (2016)	Fuegian Andes	16	15	15

Elevation (m.a.s.l.) is provided as a minimum to maximum range in the observed period. The zones are consistent with those of Figure 1.

Mutz and others, 2021). Statistical temperature downscaling should include at least one predictor reflecting temperature and one circulation-related predictor (Huth, 2002). Suitable predictors for precipitation downscaling are mid-tropospheric geopotential height, humidity (Cavazos and Hewitson, 2005) and dew-point temperature depression (Charles and others, 1999). We also include zonal and meridional wind component at 850 hPa level and the Antarctic Oscillation (AAO) due to their known control on precipitation in Patagonia (Silvestri and Vera, 2003; Garreaud and others, 2013). Inclusion of the latter is also supported by its correlation with mass-balance variation in the Peruvian Andes (Kaser and others, 2003). Furthermore, several studies suggest a significant influence of El Niño-Southern Oscillation (ENSO) on Andean low-latitude glaciers (Ribstein and others, 1995; Kaser and others, 2003; Francou and others, 2004; Rabatel and others, 2013; Maussion and others, 2015; Veettil and others, 2016), and a relationship between the Pacific Decadal Oscillation (PDO) and glacier fluctuation for tropical glaciers of the Andes (Veettil and others, 2016). Indices for both are also included in our set of potential predictors. The complete set of potential predictors thus comprises indices of the AAO, ENSO and PDO, as well as regional means of *2m air temperature (t)*, *precipitation (p)*, *mean sea level pressure (slp)*, *zonal wind speed at 850 hPa (u)*, *meridional wind speed at 850 hPa (v)*, *dewpoint temperature depression at 850 hPa (dpd)* and *geopotential height at 700 hPa (h)*. The predictors are calculated as annual and seasonal values. In this study, seasons refer to times of accumulation (April–September) and ablation (October–March).

The regional means that serve as predictors are anomalies of spatial averages that are obtained by averaging the grid points within a 500 km radius around each glacier. An overview on methods to calculate an index of the AAO (*aaoi*) is given in Ho and others (2012). We adopt the method of the National Oceanic and Atmospheric Administration (NOAA) based on empirical orthogonal function (EOF) analysis (NOAA, 2005): The monthly mean 700 hPa height anomaly field south of 20°S is projected onto the loading pattern of the AAO. The loading pattern is the first mode of variability obtained by EOF analysis over the monthly mean 700 hPa height field poleward from 20°S. The seasonal cycle is removed from the data before performing the EOF analysis. In order to account for a spherical Earth, the gridded climate data are weighted by the square-root of the cosine of latitude. An index of the PDO is obtained in a similar way. Sea surface temperature anomalies north of 20°N are

projected onto the loading pattern of the *Pacific Decadal Oscillation Index (pdoi)* (Garreaud and others, 2009). The loading pattern is obtained by performing an EOF analysis on the sea surface temperature anomalies north of 20°N. We use the *Multivariate ENSO Index (mei)* as an index for ENSO (see Wolter and Timlin, 1993, for an initial definition). The *mei* is constructed following Wolter and Timlin (2011) with slight modifications following Mutz and others (2021).

### 2.3.2 Correlation analysis

Correlation analyses aid in the first assessment of the suitability of constructed atmospheric variables as predictors of glacier mass-balance in South America. We use the Pearson correlation coefficient (PCC), which is a common measure for linear statistical dependence of two random variables (Von Storch and Zwiers, 2003; Wilks, 2006). The PCC or  $r$  is calculated for each glacier mass-balance record  $\vec{y}$  and potential predictor  $\vec{x}$  as:

$$r_{yx} = \frac{\sum_{i=1}^n (y_i - \bar{y})(x_i - \bar{x})}{\sqrt{\sum_{i=1}^n (y_i - \bar{y})^2 \sum_{i=1}^n (x_i - \bar{x})^2}} \quad (1)$$

where  $y_i$ ,  $x_i$  are the  $i$ -th element of the  $i = 1, \dots, n$  elements in  $\vec{y}$  and  $\vec{x}$  respectively.  $\bar{y}$  and  $\bar{x}$  are the means of the  $n$  elements in  $\vec{y}$  and  $\vec{x}$  respectively. The PCC has values between  $-1$  and  $1$  where  $1$  denotes a strong positive, and  $-1$  a strong negative linear dependence of  $\vec{y}$  and  $\vec{x}$ . We use the same equation to determine predictor multicollinearity (see Model training section). The correlation between annual and seasonal mass-balance records is determined by the same calculation performed on moving 10-year time windows (e.g. Mutz and others, 2015). The statistical significance of  $r$  is calculated with a beta distribution on the interval  $-1, 1$  and shape parameters  $a = b = n/2 - 1$  (Wilks, 2006). The resulting value  $p$  gives an estimate on the probability that two non-related random vectors with the assumed distribution yield the same value of  $r$  (Wilks, 2006). We use the common significance threshold of  $\alpha \leq 0.05$ .

### 2.3.3 Model training

We construct two sets of EGMs. The models of the first set predict the annual mass-balance ( $B_a$ ), while the models of the second set predict the glaciers' mass-balance ( $B_w$ ) and summer mass-balance ( $B_s$ ) separately. We train the first set of EGMs for each glacier that fulfills at least the computational requirements of our approach and construct the seasonal ( $B_w$  and  $B_s$ ) empirical glacier mass-

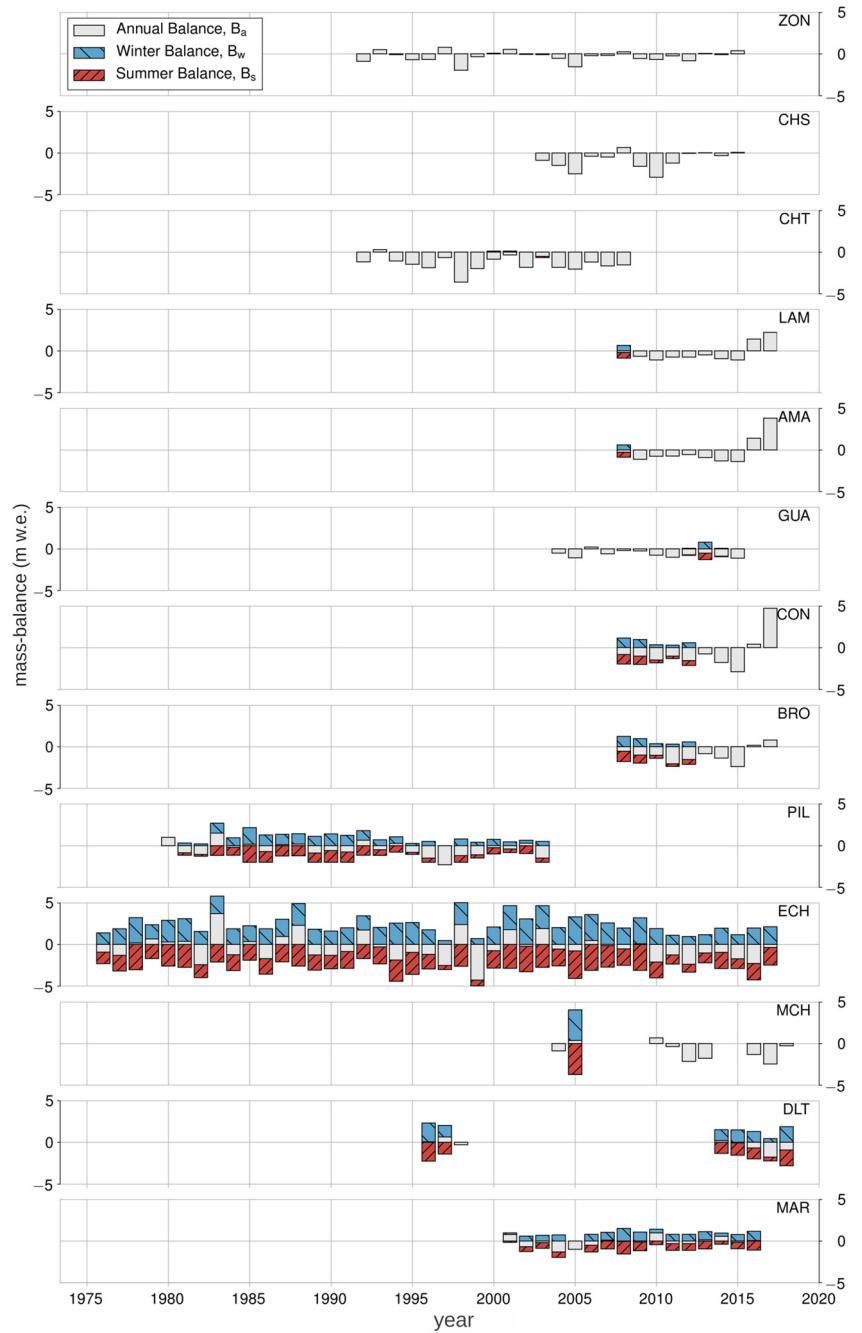


**Fig. 2.** Glacier mass-balance records used in this study. Annual mass-balance ( $B_a$ ) is shaded in grey, winter mass-balance ( $B_w$ ) is shaded in blue, and summer mass-balance ( $B_s$ ), the difference between  $B_a$  and  $B_w$ , is shaded in red. For some glaciers, only annual data exist. Notable differences in mass turnover can be observed for the glaciers with seasonal mass-balance data.

balance models (EGMs) for glaciers with sufficiently long summer and winter mass-balance records. This results in a total of 13 different annual mass-balance models (for all of the study’s glaciers except Agua Negra (AGN), Azufre (AZF) and Alerce (ALC)), and three winter mass-balance ( $B_w$ ) and summer mass-balance ( $B_s$ ) models for the glaciers Piloto Este (PIL), Echaurren Norte (ECH) and Martial Este (MAR). The EGMs are constructed by applying a classic empirical-statistical down-scaling (ESD) approach (e.g. Mutz and others, 2021) directly to glacier mass-balance records, as successfully done by Mutz and others (2015) and Schöner and Böhm (2007). The premise of this method is that the mass-balance of a glacier is linearly related to one or several variables that describe the large-scale state of the atmosphere. In its simplest form, the relationship can be summarised as:

$$\vec{Y} = f(\vec{X}) + \epsilon \tag{2}$$

where  $\vec{Y}$  is the predictand (i.e. mass-balance),  $\vec{X} = X_1, X_2, \dots, X_p$  are the predictor variables (i.e. climate variables) and  $\epsilon$  is the remaining variance that cannot be explained by  $\vec{X}$ . The assumed linearity of the regression problem is described by:

$$f(\vec{X}) = \vec{a} \cdot \vec{X} + b \tag{3}$$

where  $\vec{a} = a_1, a_2, \dots, a_p$  are the regression model coefficients of the different predictors and  $b$  is the regression intercept. These parameters make up the core of the EGMs. Their optimal values are determined in a stepwise multiple linear regression with forward selection (Von Storch and Zwiers, 2003). The stepwise multiple regression is performed within a  $k$ -fold cross-validation setting (Michaelsen, 1987; Zhang, 1993). In each fold, the data are split into training and testing subsets. The regression is conducted on the training subset, while the model’s improvement is evaluated on the testing subset. Since we train our EGMs for each glacier individually, the glacier’s training and testing data

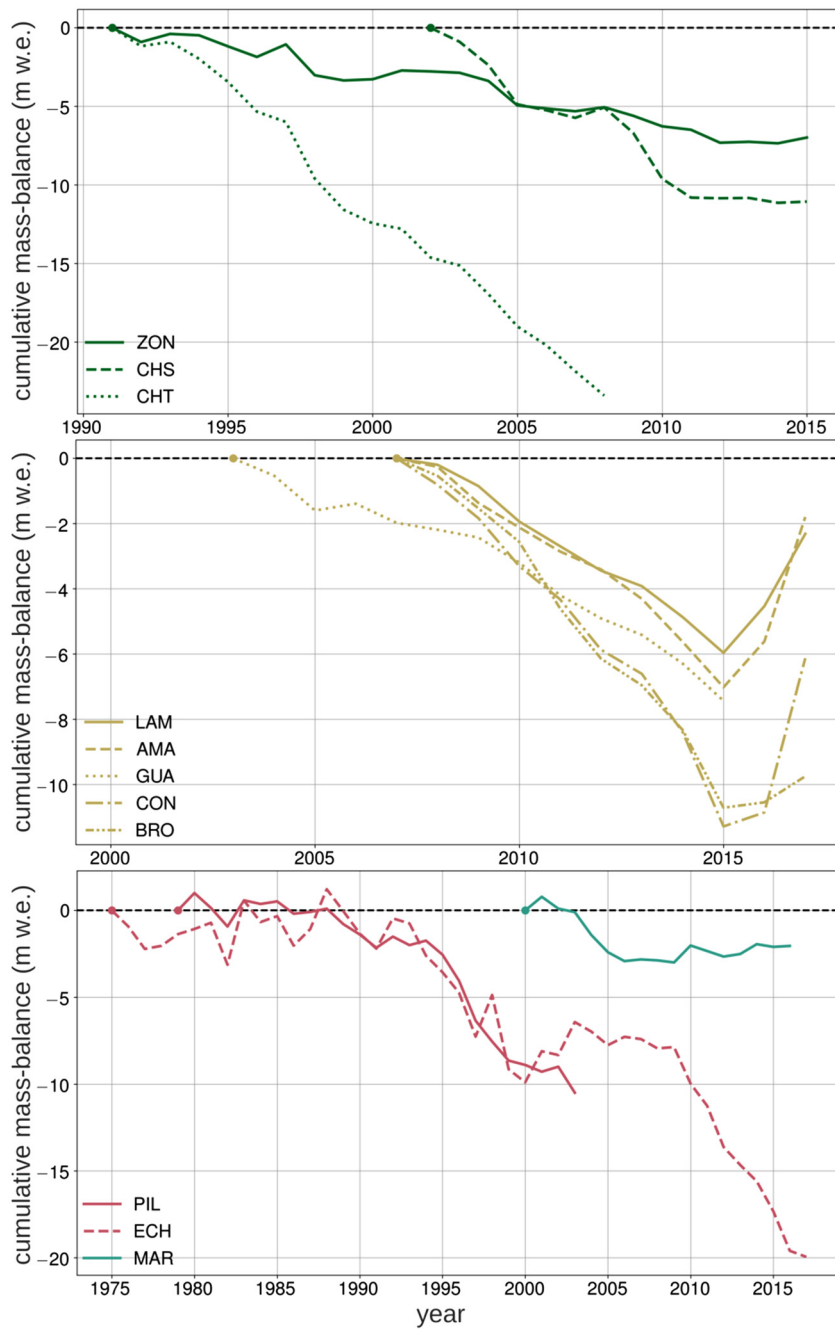


**Fig. 3.** Cumulative annual mass-balances of the glaciers used in this study. The cumulative balances are set to zero at the beginning of the measurement for each record. Colour coding corresponds to the glaciological zones presented in Figure 1.

subsets are taken from the same glacier's mass-balance time series only. The number of folds  $k$  is set to be two-thirds of the total number of data points over which the model is fitted. From the resulting  $k$  sets of model parameters  $\vec{a}$  and  $b$ , final model parameters  $\hat{a}$  and  $\hat{b}$  are calculated after the cross-validation. Final model parameters in  $\hat{a}$  are computed for each parameter as arithmetic means of the  $k$  values of the cross-validation folds. In order to ensure the robustness of the model, only predictors that contributed to the improvement of the model in at least 20% of the  $k$  cross-validation folds are included in the final model. The other parameters are discarded and set to zero.

In order to reduce potential problems arising from predictor multicollinearity, predictors are pre-filtered based on a correlation analysis (see section Correlation analysis, Eqn (1)). For each climate variable, only the predictor time series (annual, ablation or accumulation) that is best correlated with the predictand is included in the set of potential predictors. The other two seasonal predictor time series are no longer considered. The chosen potential predictors are then correlated with each other for further filtering. If

a predictor is significantly ( $\alpha \leq 0.05$ ) or highly (with  $r \geq 0.5$ ) correlated to a predictor showing higher correlation to the predictand, the former is removed from the set of predictors.

The annual mass-balance ( $B_a$ ) of a glacier can be predominantly controlled by either  $B_w$  or  $B_s$ , depending on the glacier's regime. This can change over time (e.g. Winkler and Nesje, 2009; Mutz and others, 2015), which in turn may compromise pure  $B_a$  models. We therefore additionally construct  $B_w$  and  $B_s$  models for three of glaciers that have sufficiently long  $B_w$  and  $B_s$  records (PIL, ECH and MAR). In order to allow a more merited discussion of the potential limitations of the  $B_a$  models, we conduct correlation analyses of  $B_w$  and  $B_s$  with  $B_a$ , which is expected to reveal changes in the predominant seasonal control on  $B_a$ . We use the Pearson correlation coefficient (PCC) as described in section Correlation analysis (Eqn (1)). For models of seasonal mass-balance ( $B_w$  and  $B_s$ ), the predictor time series for the irrelevant season is omitted. Thus, ablation season predictor time series are omitted in  $B_w$  modelling and vice versa.

**Table 2.** Overview of all climate predictors and their acronyms used in this study

Name	Acronym
Near surface (2m) air temperature	<i>t</i>
Precipitation rate	<i>p</i>
Zonal wind speed at 850 hPa	<i>u</i>
Meridional wind speed at 850 hPa	<i>v</i>
Geopotential height at 700 hPa	<i>h</i>
Dew point depression at 850 hPa	<i>dpd</i>
Sea level pressure	<i>slp</i>
Multivariate ENSO Index	<i>mei</i>
Antarctic Oscillation Index	<i>aaoi</i>
Pacific Decadal Oscillation Index	<i>pdoi</i>

### 2.3.4 Model evaluation

The constructed, final model consists of transfer functions between glacier mass-balance and robust large-scale climate predictors. These EGMs are then used to generate predictions ( $\hat{Y}$ ) for the observed mass-balance data  $\vec{Y}$ . The model's performance is assessed in several ways.

The coefficient of determination  $R^2$  expresses the fraction of the predictand variance that can be explained by the models. More specifically, it is a measure of how much better the model represents  $\vec{Y}$  compared to how much the mean  $\bar{y}$  represents  $\vec{Y}$  (Wilks, 2006). The coefficient of determination is defined as:

$$R^2 = 1 - \frac{SSR}{SST} = 1 - \frac{\sum_{i=1}^n (y_i - \hat{y}_i)^2}{\sum_{i=1}^n (y_i - \bar{y})^2} \quad (4)$$

where  $SSR$  is the sum of squared residuals and  $SST$  is the total sum of squares.  $y_i$  and  $\hat{y}_i$  are the  $i$ -th elements of the  $i = 1, \dots, n$  elements in  $\vec{Y}$  and  $\hat{Y}$  respectively.  $\bar{y}$  is the mean of the  $n$  elements in  $\vec{Y}$ .  $R^2$  can range from  $-\infty$  to 1, where a value of 1 indicates a perfect fit, and a value of 0 indicates no improvement of the model over a simple  $\bar{y}$  model for  $\vec{Y}$ . Negative values of  $R^2$  indicate that  $\bar{y}$  represents  $\vec{Y}$  better than the predictions.

The root mean squared error ( $RMSE$ ) provides information on the magnitude of the error of the prediction. It is a measure of misfit between predictions  $\hat{Y}$  and observations  $\vec{Y}$ . It is calculated as:

$$RMSE = \sqrt{\frac{1}{n} \sum_{i=1}^n (\hat{y}_i - y_i)^2} \quad (5)$$

where  $\hat{y}_i$  is the  $i$ -th element of the  $i = 1, \dots, n$  elements in  $\hat{Y}$ , and  $y_i$  is the mean of the  $n$  elements in  $\vec{Y}$ . The  $RMSE$  can be interpreted in the same physical units as  $\vec{Y}$  and gives a typical magnitude for the prediction error (Wilks, 2006). The smaller the  $RMSE$  is, the better the model represents the data in  $\vec{Y}$ .

The two metrics  $R^2$  and  $RMSE$  are calculated for the entire observational period if the mass-balance records are too short to subdivide into completely separate training and testing data subsets. For glaciers with mass-balance records of at least 20 years, additional experiments are performed in which the individual models are fitted on the first and second half of the available record (e.g. Mutz and others, 2021).

The importance and explanatory power of a predictor is evaluated in the course of the forward selection algorithm. In every forward selection step, the algorithm calculates the improvement of  $R^2$  that can be achieved by including the predictor. A predictor is included in the final model if it frequently contributes to a significant increase of  $R^2$  in each of the  $k$  cross-validation folds. The  $k$  values of  $R^2$  are averaged for the included (robust) predictors to yield the final estimate of average explained variance. The reader

is referred to Von Storch and Zwiers (2003) and Wilks (2006) for more details on the stepwise multiple regression with forward selection, and to Mutz and others (2015) for more details on its application to glacier mass-balance modelling.

## 3. Results

### 3.1 Correlation analyses

There are four distinct groups of glaciers with regard to the correlation of their glacier-wide mass-balances with potential predictors (Fig. 4). The first group consists of the Outer Tropics glaciers in Bolivia (Zongo (ZON), Charquini Sur (CHS), Chacaltaya (CHT)) which are all significantly negatively correlated to summer 2 m air temperature ( $t$ ) ( $\alpha \leq 0.05$ ). The second group includes the subtropical glaciers of the Desert Andes (Los Amarillos (LAM), Amarillo (AMA), Guanaco (GUA), Conconta Norte (CON), Brown Superior (BRO)). These are characterised by high positive ( $\sim 0.5 - 0.9$ ) correlation coefficients for  $B_a$  and zonal wind speed at 850 hPa ( $u$ ), and slightly lower, negative correlation coefficients for  $B_a$  and meridional wind speed at 850 hPa ( $v$ ). The third group consists of the Central Andes glaciers PIL and ECH. Their annual mass-balances show significant positive correlation with precipitation ( $p$ ) and  $u$ , and significant negative correlation with mean sea level pressure ( $slp$ ),  $v$ , dew-point temperature depression at 850 hPa ( $dpd$ ) and geopotential height at 700 hPa ( $h$ ). The  $B_a$  of ECH is also significantly positively correlated with the Multivariate ENSO Index ( $mei$ ), Antarctic Oscillation Index ( $aaoi$ ) and  $u$ . The fourth group only consists of the glacier MAR, which is located in Tierra del Fuego. MAR's correlation pattern is similar to that of PIL and ECH. However, in contrast to PIL and ECH, there is a significant negative correlation with  $t$ , and a positive correlation with  $v$ . The remaining glaciers of the Desert Andes (AGN), Central Andes (AZF), Lakes District (Mocho Choshuenco SE (MCH)) and Patagonian Andes (ALC and De Los Tres (DLT)) did not yield significant results.

The winter mass-balances of PIL, ECH and MAR show a correlation pattern comparable to that of  $B_a$ . The main difference is the lack of a significant negative correlation with  $t$  for the glacier MAR. The summer mass-balance of PIL is not significantly correlated to any predictor variable. For ECH, the correlation with the respective predictors is generally weaker for  $B_s$  than for  $B_w$ . The  $B_s$  of MAR is significantly negatively correlated with  $t$ . Neither annual nor seasonal mass-balance of any glacier are significantly correlated with the  $pdoi$ . The correlation between seasonal mass-balances and  $B_a$ , computed from moving 10-year time windows for glaciers PIL, ECH and MAR, reveals a (mostly) stronger correlation of  $B_w$  with  $B_a$  for PIL, consistently stronger correlation of  $B_w$  with  $B_a$  for ECH, and a consistently stronger correlation of  $B_s$  with  $B_a$  for MAR (Fig. 5). For the glacier ECH, the correlation of seasonal mass-balances with  $B_a$  weakens from the calculation window 2000–2010 onward. The correlation coefficient values for  $B_s$  with  $B_a$  are more severely reduced (from  $\sim 0.75$  to  $\sim 0.4$ ) and cease to be significant (Fig. 5).

### 3.2 Empirical glacier mass-balance models

EGM performance varies significantly between glaciers. For  $B_a$  models, the  $RMSE$  ranges between 0.24 and 1.23 m w.e. with a mean of  $\sim 0.61$  m w.e. The  $R^2$  values lie between 0.15 and 0.74 and generate a mean of  $\sim 0.45$ .  $r_{yy}$  is significant ( $\alpha \leq 0.05$ ) for all  $B_a$  models.

The four different groups identified by correlation analyses are also reflected in the estimated contribution to the total explained variance ( $R^2$ ) by each predictor for each glacier (Fig. 6). Regional

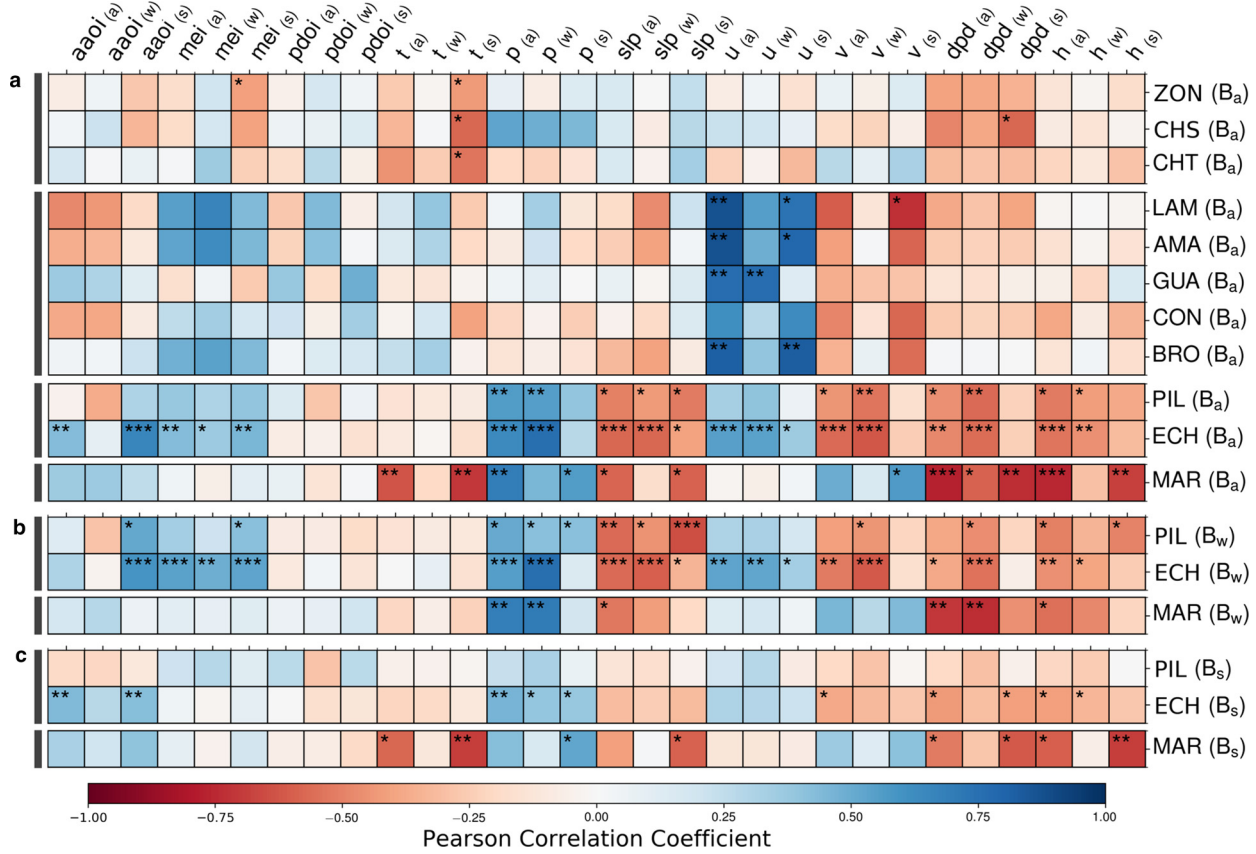


**Fig. 4.** Pearson correlation coefficients between the predictors (columns) and mass-balances of the glaciers (columns) of this study that meet the requirements for this analysis. Results are shown for (a) Outer Tropics (top), Desert Andes, Central Andes and Fuegian Andes (bottom) glacier annual mass-balance ( $B_a$ ), (b) Central Andes (top) and Fuegian Andes (bottom) glacier winter mass-balance ( $B_w$ ) and (c) Central Andes (top) and Fuegian Andes (bottom) glacier summer mass-balance ( $B_s$ ) separately. Seasonal mass-balances are only evaluated for the glaciers PIL, ECH and MAR due to lack of sufficiently long seasonal mass-balance records for the other glaciers. The predictors (Antarctic Oscillation Index (aaol), Multivariate ENSO Index (mei), Pacific Decadal Oscillation Index (pdo), 2 m air temperature (t), precipitation (p), mean sea level pressure (slp), zonal wind speed at 850 hPa (u), meridional wind speed at 850 hPa (v), dew-point temperature depression at 850 hPa (dpd) and geopotential height at 700 hPa (h) are calculated for different months and seasons as described in section Predictor construction. Significance levels (from two-tailed tests) are denoted with asterisks in the figure ( $\alpha \leq 0.001$ : \*\*\*;  $\alpha \leq 0.01$ : \*\*;  $\alpha \leq 0.05$ : \*).

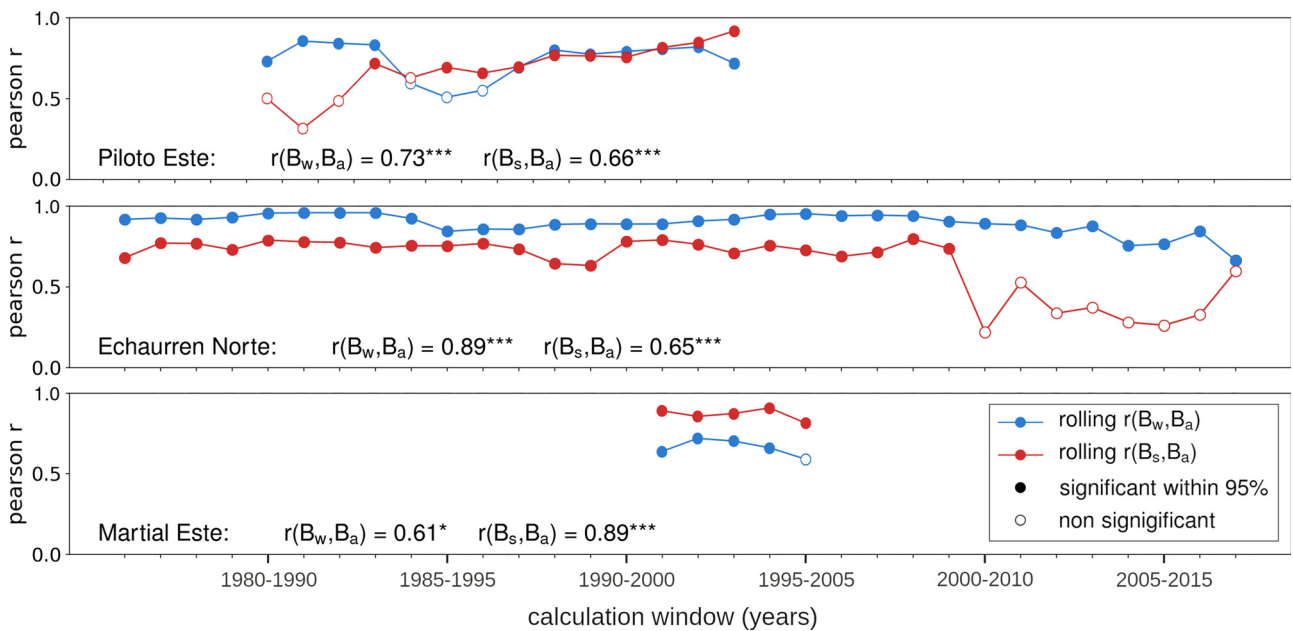


**Fig. 5.** Correlations between winter mass-balance and annual mass-balance  $r(B_w, B_a)$  and summer mass-balance and annual mass-balance  $r(B_s, B_a)$  for the glaciers PIL (top), ECH (middle) and MAR (bottom). The plots show correlation coefficients calculated in 10-year moving windows. Filled dots indicate correlations that are significant ( $\alpha \leq 0.05$ ) and empty dots indicate non-significant correlations. The correlation coefficients calculated over the total records are listed at the bottom of the plot for each glacier ( $\alpha \leq 0.001$ : \*\*\*;  $\alpha \leq 0.01$ : \*\*;  $\alpha \leq 0.05$ : \*).

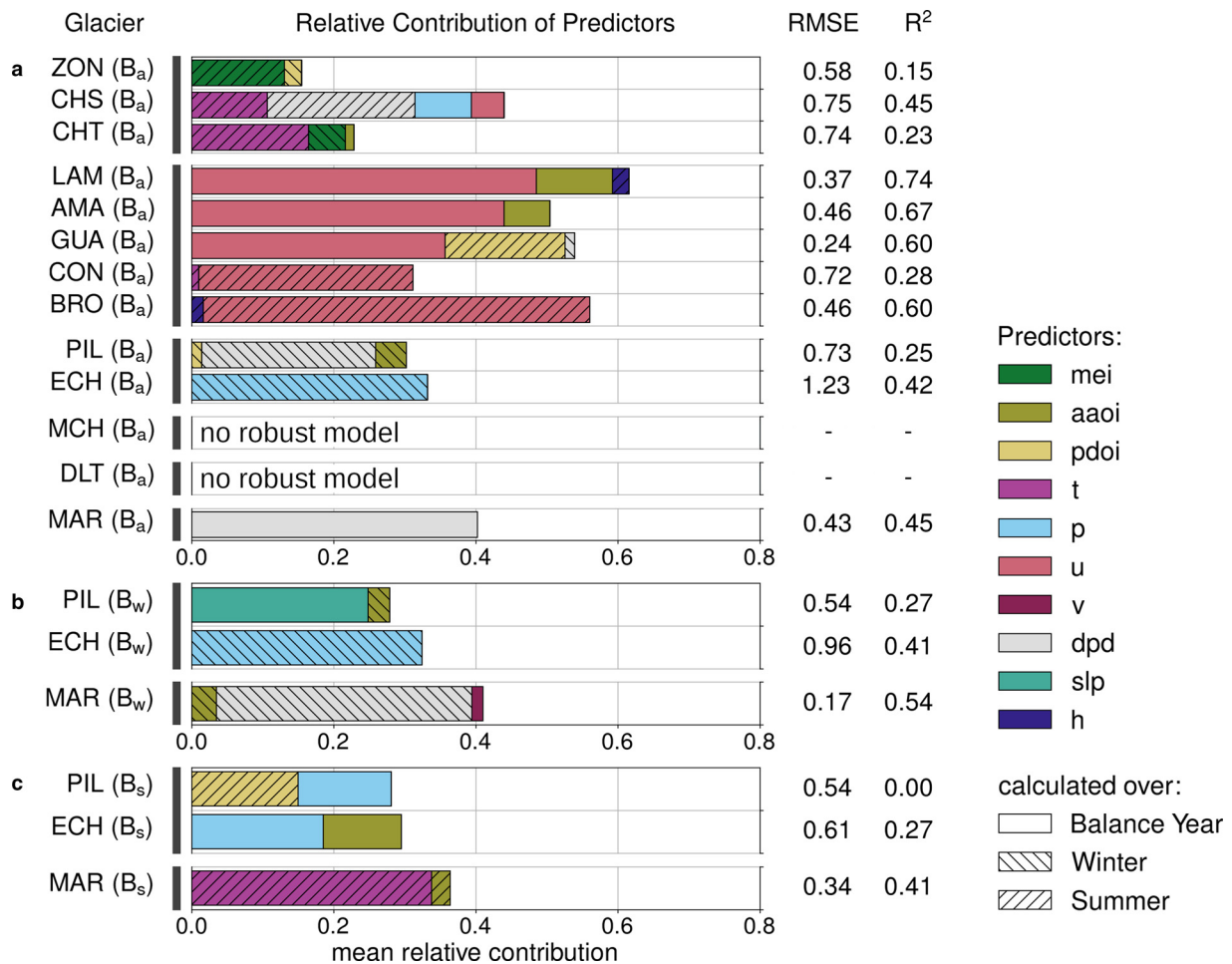


**Fig. 6.** Model skill measures (*RMSE* and *R*<sup>2</sup>) and mean relative contribution of the different predictors (*Antarctic Oscillation Index (aaoi)*, *Multivariate ENSO Index (mei)*, *Pacific Decadal Oscillation Index (pdoi)*, *2 m air temperature (t)*, *precipitation (p)*, *mean sea level pressure (slp)*, *zonal wind speed at 850 hPa (u)*, *meridional wind speed at 850 hPa (v)*, *dew-point temperature depression at 850 hPa (dpd)* and *geopotential height at 700 hPa*) to the total explained variance (*R*<sup>2</sup>) for (a) the annual mass-balance of the Outer Tropics (top), Desert Andes, Central Andes, Lakes District, Patagonian Andes and Fuegian Andes (bottom) glaciers, (b) the winter mass-balance of the Central Andes (top) and Fuegian Andes (bottom) glaciers, and (c) the summer mass-balance of the Central Andes (top) and Fuegian Andes (bottom) glaciers. The *RMSE* and *R*<sup>2</sup> values are based on the final mass-balance regression models trained with ERA-Interim over the temporal overlap of ERA-Interim and available B<sub>a</sub> record. The hatching of the bars represents the season over which the predictor is calculated. If the model selection algorithm fails to find a robust model, i.e. if no predictor passes the 40% threshold of being nonzero in the cross-validation loops, this is indicated in the figure.

means of *t* and the El Niño-Southern Oscillation (ENSO) index are only chosen as robust B<sub>a</sub> predictors for the Outer Tropics glaciers (ZON CHS and CHT) and contribute to the total explained variance with ~5 to ~15%. The annual mass-balance of the Desert Andes glaciers (LAM, AMA, GUA, BRO) is mostly explained by (*u*). This predictor is able to explain between ~35% (CON) and ~55% (BRO) of the predictand variance.

The annual mass-balance variance of the glaciers of the Central Andes (PIL and ECH) and Tierra del Fuego (MAR) is mostly explained by regionally averaged anomalies of *p* and *dpd*.

The *RMSE* values for the seasonal models of PIL, ECH, MAR are smaller than for the B<sub>a</sub> models. The *R*<sup>2</sup> values for B<sub>w</sub> and B<sub>s</sub> models are similar and lower than those of the B<sub>a</sub> models, respectively. The B<sub>s</sub> model of glacier PIL shows no improvement over the prediction by the mean. The selected predictors of the seasonal mass-balance models are partly different from the predictors selected for the B<sub>a</sub> models. The dominant predictors for B<sub>w</sub> show the most overlap with the dominant predictors for B<sub>a</sub>. There are only slight differences between B<sub>a</sub> that is modelled directly and B<sub>a</sub> that is constructed from its modelled B<sub>s</sub> and B<sub>w</sub> components. The three skill metrics are in the same ranges for the two differently modelled annual mass-balances and differ by ≤ ±10% for glaciers ECH and MAR and ≤ ±30% for glacier MAR. However,

**Table 3.** Skill metrics (*R*<sup>2</sup> and *RMSE*) calculated from (1) observed B<sub>a</sub> and directly modelled  $\hat{B}_a$  ( $\hat{y} = \hat{B}_a$ ), and (2) observed B<sub>a</sub> and modelled  $\hat{B}_a$  calculated from the modelled B<sub>w</sub> and  $\hat{B}_s$  components ( $\hat{y} = \hat{B}_w + \hat{B}_s$ ) for the glaciers PIL, ECH and MAR

Glacier	No. of records (B <sub>a</sub> , B <sub>w</sub> , B <sub>s</sub> )	Skill metric	$\hat{y} = \hat{B}_a$	$\hat{y} = \hat{B}_w + \hat{B}_s$
PIL	24, 24, 24	<i>RMSE</i>	0.77	0.75
		<i>R</i> <sup>2</sup>	0.17	0.20
ECH	42, 42, 42	<i>RMSE</i>	1.23	1.18
		<i>R</i> <sup>2</sup>	0.42	0.46
MAR	16, 15, 15	<i>RMSE</i>	0.43	0.43
		<i>R</i> <sup>2</sup>	0.45	0.45

skill metrics values are generally slightly better (lower *RMSE* and higher *R*<sup>2</sup>) for the mass-balance that is modelled from the seasonal mass-balances. An overview of the seasonal and annual performance metrics is provided in Table 3. The model performance metrics are higher for models trained over parts of the mass-balance records than for the models trained on the full mass-balance records if calculated from the training period. However, their prediction skills, as evaluated using completely independent data from the complementary half of mass-balance record, is significantly lower. Most of the models trained on these smaller data subsets have prediction skills with values of *R*<sup>2</sup> close to zero or even negative.

## 4. Discussion

### 4.1 Predictors of South American glacier mass-balance

Results of correlation analyses and predictor selection during EGM training give insights into the potential of different synoptic-scale climate variables as predictors for South American glacier mass-balance changes. Since considered predictors are chosen based on their physical relevance, our results may also highlight the relative importance of different atmospheric movements or processes for the studied glaciers. The computed correlation coefficients and predictor selection in EGM training reveal four distinct groups of glaciers. These comprise (1) Outer Tropics glaciers in Bolivia (ZON, CHS, CHT), (2) Desert Andes glaciers at  $\sim 29^\circ\text{S}$  (LAM, AMA, GUA, CON, BRO), (3) Central Andes glaciers at  $\sim 33^\circ\text{S}$  (PIL, ECH) and (4) the glacier of Tierra del Fuego (MAR). This grouping is consistent with the findings of Sagredo and Lowell (2012) and the glaciological zones proposed by Lliboutry (1998), Barcaza and others (2017), and Zalazar and others (2020) (see also Fig. 1 and Table 1). Since no information about the glaciological zones was included in our analyses, our results provide independent evidence that confirm the merits of this classification for South American glaciers.

#### 4.1.1 Outer tropics glaciers

Our findings identify summer  $2\text{ m}$  air temperature ( $t$ ), the Multivariate ENSO Index ( $mei$ ) and summer dew-point temperature depression at 850 hPa ( $dpd$ ) as decent predictors for  $B_a$  of Outer Tropics glaciers. This glaciological zone corresponds to group 2.2 cluster (Sagredo and Lowell, 2012), which is characterised by monthly temperature and precipitation means of  $\sim 0$  to  $\sim 3^\circ\text{C}$  and  $\sim 0$  to  $\sim 140$  mm, respectively (Sagredo and Lowell, 2012). Generally, the outer tropical hydrological year can be divided into a dry season (austral winter) and a wet season (austral summer) (e.g. Francou and others, 1995; Sicart and others, 2007), and both accumulation and ablation are highest in the wet season (e.g. Sicart and others, 2007). This seasonal (summer) bias is reflected in our results. Previous studies identify the short and longwave radiation budget, which is closely linked to albedo, as an important determinant for Outer Tropics ablation (Rabatel and others, 2013). Temperature integrates accumulation and ablation processes, as it is not only a measure of latent heat flux (long wave radiation budget), but also controls albedo (short wave radiation budget) by determining if precipitation falls as albedo-increasing solid (snow), thus adding mass to the glacier, or liquid (Rabatel and others, 2013). It can thus be a predictor for mass-balance changes on the annual scale. Our identification of temperature as the most important predictor is therefore consistent with our knowledge of underlying mechanisms, especially given that the Outer Tropics glacier models are trained using  $B_a$  records. The onset of the wet season is important to Outer Tropics glacier mass-balance as highest melt rates occur at the end of the dry season when low values of glacier albedo and high values of solar irradiance prevail (Rabatel and others, 2013). With the onset of the wet season, solar irradiance is reduced due to convective clouds, and albedo is increased by frequent snowfall. This special importance of seasonal distribution of precipitation may in parts explain the inclusion of summer dew point temperature as an important predictor in our models. Wagnon and others (2001) show a time lag in the onset of the rain period during El Niño events, which results in negative mass-balance anomalies. This can explain the selection of  $mei$  as a robust predictor for the  $B_a$  of glacier CHS and the significant correlation  $mei$  to the annual mass-balance of glacier ZON.

#### 4.1.2 Desert Andes glaciers

We identify zonal wind speed at 850 hPa ( $u$ ), the Antarctic Oscillation Index ( $aoi$ ) and Pacific Decadal Oscillation Index

( $pdoi$ ) as strong predictors for the mass-balance of our Desert Andes glaciers. These are located at high altitudes with mean annual temperature below  $0^\circ\text{C}$ , which causes perennial solid precipitation (Rabatel and others, 2011). Monthly mean precipitation ranges from  $\sim 10$  to  $\sim 50$  mm (Sagredo and Lowell, 2012). Ablation mainly occurs via sublimation and only a small fraction of total ablation is achieved by melting (MacDonell and others, 2013). Mass-balance variation are therefore predominantly controlled by changes in precipitation (Rabatel and others, 2011). Precipitation in these latitudes is primarily controlled by frontal activity in winter and convective storms in summer (MacDonell and others, 2013). Since zonal wind speeds at 850 hPa are a measure of frontal activity, they are also related to precipitation variability. The choice of summer  $u$  as the main predictor for glaciers CON and BRO suggests the influence of the low-level jet. The two glaciers are located east of the other Desert Andes glacier (Fig. 1) in a region prone to summer snowfall events due to moisture transport by the low-level jet (Marengo and others, 2004). This is consistent with the findings for the corresponding group of glaciers in Sagredo and Lowell (2012). The influence of the Antarctic Oscillation (AAO) on LAM and AMA in our results can likely be explained by high latitude forcing for precipitation variability in northern-central Chile (Vuille and Milana, 2007) and the extent of regional impacts of the Southern Annular Mode (Gillett and others, 2006). The identification of the summer  $pdoi$  as a predictor for Desert Andes glaciers is supported by findings that precipitation anomalies in the same region are also associated with variations in Pacific Decadal Oscillation (PDO) (Quintana and Aceituno, 2012). However, we note that the true scale of the influence of the PDO cannot be estimated from the relatively short glaciological time series used in this study. In summary, the predictors we identified represent important controls on precipitation in these latitudes and are thus consistent with underlying mechanisms for ablation and accumulation.

#### 4.1.3 Central Andes glaciers

In contrast to the glaciers of the Outer Tropics and the Desert Andes, the seasonality of the mass-balance year for the glaciers ECH and PIL (located at  $\sim 33^\circ\text{S}$ ) is more accentuated (Pellicciotti and others, 2008; Rabatel and others, 2011; Masiokas and others, 2016; Ayala and others, 2017). More specifically, monthly temperature and precipitation means range from  $\sim -5$  to  $\sim 5^\circ\text{C}$  and  $\sim 10$  to  $\sim 160$  mm, respectively (Sagredo and Lowell, 2012). Most of the total annual precipitation occurs in winters (Masiokas and others, 2016) while the summers are very dry with often completely absent precipitation (Pellicciotti and others, 2008). Our results suggest that PIL and ECH mass-balances are primarily controlled by regional precipitation or dew point temperature, which can serve as a proxy for precipitation. This is in agreement with the findings of Rabatel and others (2011) and Masiokas and others (2016), who demonstrate that the mass-balance of ECH is driven by changes in precipitation, while temperature changes play a secondary role. The significant correlation with other predictors ( $aoi$ ,  $mei$ ,  $slp$ ,  $h$ ) with  $B_a$  of ECH (and partly PIL) may be explained by their effects on precipitation variability. Since precipitation anomalies are controlling  $B_a$ , accumulation is found to be more important than ablation for ECH and PIL. This is additionally supported by weak correlations of the predictor variables with the  $B_s$  series of ECH and PIL and stronger correlations of the annual mass-balances with  $B_w$  than with  $B_s$  (see Fig. 5). The decoupling of ECH's  $B_s$  and  $B_a$ , and the weakening correlation of  $B_w$  with  $B_a$  from the calculation window 2000–2010 onward (Fig. 5) temporally coincides with the Central Chile Mega Drought (Garreaud and others, 2019). Given that the primary control for ECH's mass-balance is

precipitation, a prolonged drought can break down the otherwise strong empirical relationship. The glacier AZF does not have a sufficiently long mass-balance record to yield meaningful results.

#### 4.1.4 Lakes District and Patagonian glaciers

We were unable to identify robust predictors for mass-balance of glaciers in the Lakes District (MCH) and more southern Patagonia (ALC and DLT). The glacier ALC had to be excluded from analysis entirely due to the absence of mass-balance records that temporally overlap with the reanalysis data. MCH and DLT likely still have too few measurements in succession (see Fig. 2) to produce meaningful results for the approach used in this study.

#### 4.1.5 Fuegian Andes glaciers

The southernmost glacier MAR belongs to the group of glaciers in the Fuegian Andes, which experience monthly mean temperatures of  $\sim -1$  °C in winter to  $\sim 5$  °C in summer and precipitation rates of  $\sim 70$  mm per month with low seasonal variation (Sagredo and Lowell, 2012). We identify *d<sub>pd</sub>* and summer *t* as the best predictors for mass-balance changes of MAR. Furthermore, precipitation anomalies correlate strongly with  $B_w$  and  $B_a$ . This is consistent with findings by Strelin and Iturraspe (2007), who attribute positive and negative mass-balance variations of the glacier MAR to humid-cool summer seasons and dry-warm years respectively. Precipitation anomalies are excluded from the mass-balance models of MAR in favour of the inclusion of *d<sub>pd</sub>*. This may be due to better representation of relevant precipitation variability by *d<sub>pd</sub>* at the location of the glacier.

### 4.2 Empirical glacier mass-balance models for South America

The  $B_a$  models of this study perform reasonably well with average performance metrics values  $RMSE \approx 0.6$  m w.e. and  $R^2 \approx 0.5$ . We discuss these further in context of similar studies: Masiokas and others (2016) and Buttstädt and others (2009) modelled net  $B_a$  in the same area thus allow a direct comparison to our results (Table 4). Schöner and Böhm (2007) and Mutz and others (2015) adopted similar modelling techniques and thus provide a more suitable reference for evaluating the performance metrics values of our models.

Masiokas and others (2016) reconstructed the  $B_a$  for the glacier ECH based on a minimal glacier model (Marzeion and others, 2012) and two regression models using snowpack variations and local streamflow records as predictors. The minimal mass-balance model yields  $RMSE = 0.77$  m w.e., whereas the regression models yield  $RMSE = 0.91$  m w.e. and  $R^2 = 0.68$ . Buttstädt and others (2009) employed a degree-day model to simulate the mass-balance evolution of MAR from 1960 until 2099. In the calibration period, their model yields  $R^2 = 0.91$  and  $RMSE$  of 0.47 m w.e. Where comparisons are possible, the models of this study do not perform as well as previous models of Masiokas and others (2016) and Buttstädt and others (2009) (Table 4). This is expected, since our models use synoptic-scale atmospheric predictors, while the other studies either use a completely different approach, i.e. minimal mass-balance model and degree-day model, or incorporate local (proxy) data like streamflow and snowdepth records, which may hold further important information. Additionally, Buttstädt and others (2009) do not apply any cross-validation to their degree-day factor calibration. This likely leads to a higher skill in the training period, but also increases the risk of overfitting.

Some of our models can compete with the  $RMSE$  and  $R^2$  values of similarly constructed mass-balance models for glaciers in Austria (Schöner and Böhm, 2007) and Norway (Mutz and others, 2015). Even though the climatic settings are different, the comparison shows that the performance scores for a subset

**Table 4.** Comparison of skill measures (coefficient of determination ( $R^2$ ) and root mean square error ( $RMSE$ )) of models from this study and models from Masiokas and others (2016) and Buttstädt and others (2009)

Study	$R^2$	$RMSE$
This study: arithmetic mean of $B_a$ models	0.45	0.61
Masiokas and others (2016): ECH <sup>a</sup>	–	0.77
Masiokas and others (2016): ECH <sup>b</sup>	0.68	0.91
This study: $B_a$ model of ECH	0.42	1.23
Buttstädt and others (2009): MAR <sup>c</sup>	0.91	0.47
This study: $B_a$ model of MAR	0.45	0.43

<sup>a</sup>minimal mass-balance model.

<sup>b</sup>regression model.

<sup>c</sup>degree-day model.

of our glacier models are within the published range for EGMs of this type. The overall better performance by the models of previous studies can likely be attributed to the availability of more complete datasets and longer measurement records. These increase the probability of adequately capturing the relationships between synoptic-scale atmospheric variability and mass-balance changes during model training. Furthermore, they allow separate modelling of summer and winter mass-balances, which may result in better predictions of  $B_a$  (Schöner and Böhm, 2007). Overall, our results are satisfactory and speak in favour of adopting an empirical mass-balance modelling approach in South America to complement physical-numerical models.

### 4.3 Limitations and suggestions

The main shortcomings of our models can be summarised as (i) a frequent underestimation of the amplitude of predicted mass-balance variability, (ii) low performance scores for some models, (iii) uncertainties arising from mostly modelling  $B_a$  directly instead of constructing it from modelled seasonal components  $B_w$  and  $B_s$ , and (iv) the neglect of glacier dynamics that are important for predicting the long-term response to climate change. We can subdivide the limitations into the categories of data sparsity and quality, and methodological limitations.

#### 4.3.1 Data sparsity and quality

A significant problem for the approach of this study is the still very limited data base for glaciers in South America. Although we adopted methods to prevent overfitting and increase the models' robustness, the predictive capabilities of EGMs remain more uncertain when mass-balance records are not sufficiently long enough to subdivide it into completely independent training and validation period. Furthermore, the required length of the data records depends on the frequency of climatic events that affect the glacier. Therefore, the short records are particularly problematic for outer tropical glaciers, which are more directly influenced by lower frequency ENSO cycles. Pooling the data records for glaciers of the same regime and constructing more general models for a cluster of glaciers may be an option to circumvent this problem.

Due to limited glacier data records, only  $B_a$  models can currently be constructed for most of the glaciers studied here. This leads to a bias in the selection of predictor towards climatic factors in the season that is the stronger determinant of  $B_a$ . A change in the glaciological regime that leads to a shift from ablation-controlled to predominantly accumulation-controlled  $B_a$  (or vice versa) will compromise the accuracy of the EGMs. Our results indicate that this may be a problem for the  $B_a$  EGM constructed for PIL and ECH (Fig. 5).

Glaciological mass-balance records are heavily biased towards small glaciers, while most of the ice in the Andes is stored in

larger glaciers. The same is true for the glaciers of this study (see *Area* in [Table 1](#)). Furthermore, our study is unable to produce meaningful results for any of the glaciers in the Lakes District and Patagonian Andes, which contribute ~95% to the total ice volume in the major glacier regions of southern South America (Carrivick and others, 2016). The reader is advised to consider these representation issues.

The quality of relevant data is compromised by both logistical and technological factors. For example, the often difficult access to glaciers can result in delays for in-situ measurements that can ultimately lead to underestimations of winter accumulation (or summer ablation). These constitutes additional sources of uncertainty for predictions generated by EGMs.

The lack of relevant atmospheric variables in available datasets is another problem. For example, there are factors such as atmospheric black carbon from human emissions and wildfires, which can have an influence on the mass-balance of Andean glaciers (Molina and others, 2015; Magalhães and Evangelista, 2018), but cannot be considered here, because the ERA-Interim reanalysis data contain no measure for such atmospheric aerosol content.

#### 4.3.2 Methodological limitations

The strength of our approach is given by the focus on synoptic-scale controls, its cost-effectiveness, and the possibility to directly couple of the EGMs to general circulation models (GCMs). However, the EGMs should be regarded as models that complement rather than replace others, such the Open Global Glacier Model (OGGM) (Maussion and others, 2019), as they come with several notable drawbacks:

1. Predictor multicollinearity: The general underestimation of the amplitude of predicted mass-balance indicates a tendency of underfitting. The measures adopted to mitigate the problems of multicollinearity among predictors and avoid overfitting may encourage the models to generalise to a greater extent than necessary. The same measures may also create competition among predictors in the cross-validation setting to make it into the final model. In some cases, this can lead to the exclusion of important predictors (Mutz and others, 2015). The introduction of least absolute shrinkage and selection operator (LASSO) variable selection and regularisation may improve the EGMs. It is known to deal well with multicollinearity (Tibshirani, 1996) and has been successfully used for statistical climate downscaling (Hammami and others, 2012; Gao and others, 2014) and also in a glaciological context (Maussion and others, 2015). Another way to prevent problems related to multicollinearity is through the construction of new, uncorrelated predictors. This may be achieved by conducting a principal component analysis (PCA) on the set of predictor variables used in this study (see [Table 2](#)).
2. Predictor representation: It is likely that the predictors of this study do not adequately capture all important synoptic-scale atmospheric variability. This is a problem especially for low-frequency changes that are not observed in the short time covered by the mass-balance records. Possible improvements include an optimisation of the radius used in the construction of spatial means, or the fine-tuning of predictors, such as the choice of different pressure level dew-point temperature for studies with a more regional focus.
3. Assumption of linearity: Our approach uses parametric statistical models that assumes a linear relationship of glacier mass-balance and the large-scale state of the atmosphere. Problems arising from this approach may be bypassed, for example, by using a different family of regression procedures for the transfer functions, such as Random Forests (Breiman, 2001). Bolibar and others (2020) demonstrate that a deep-learning

approach is able to capture non-linear behaviour that is missed by classic regression-based techniques.

4. Temporal stationarity of transfer functions: Our approach assumes that the models' transfer functions are stationary in time. It does not take into consideration factors and mesoscale processes that likely affect mountain glaciers (Mölg and Kaser, 2011) and potentially lead to temporal instability of the transfer functions. These factors also include changes in albedo, which is important for the energy balance on the glacier and thus affects ablation. Regional mean albedo changes can be caused by different ablation zone extents if the equilibrium line altitude increases (Sagredo and others, 2014) or glaciers shrink (Gurgiser and others, 2014). Another factor are local katabatic winds that may affect ablation processes. This has been shown for the tongue of the Juncal Norte glacier (Pellicciotti and others, 2008), which is located in the same area as the glaciers ECH and PIL. For a more general discussion of spatio-temporal transferability of glacier mass-balance models, the reader is referred to Zolles and others (2019).
5. Topography and glacier dynamics: A major limitation of our models is the neglect of ice dynamics and geometry, and the implicit assumption of constant topography and glacier altitude during model training. The models are thus unable to produce the dynamic response to climate-glacier imbalances (Zekollari and others, 2020) that would change the timing and magnitude of glacier mass changes. This has serious implications for the application potential of the EGMs presented in this study. The models' transfer functions are specific to the altitude (range) of the glaciers during model training. They capture the synoptic scale climatic drivers of MB of each glacier in their topographic setting of the recent past and present-day. When altitude changes more significantly as the glacier responds to larger climate-glacier imbalances, the transfer functions of the model can no longer be regarded as valid. Therefore, the application of the EGMs presented here is only merited for predicting the short-term glacier response to changes in climate. The dynamic response may be approximated in a limited way by pooling the mass-balance data for glaciers at different altitudes in a similar glaciological zone, training altitude-specific models and implementing dynamic model selection controlled by predicted shifts in altitude. As mass-balance records continue to grow, the inclusion of topographic predictors in a deep-learning approach (e.g. Bolibar and others, 2020) represents another promising way to address this limitation.

## 5. Conclusion

We assessed the control of synoptic-scale atmospheric factors on the mass-balance of 13 glaciers in South America by means of correlation analyses. The predictive capabilities of the same factors were evaluated in the training procedures for the EGMs of each glacier. The training procedure consisted of a cross-validated stepwise multiple regression with forward selection and robustness filter for predictors. The key findings of this study are the following:

- The assessment of synoptic-scale climatic controls on South American glaciers reveal four distinct groups. The glaciers of a specific group are in geographical proximity and characterised by similar sets of important synoptic-scale predictors. The four groups can be summarised as follows: (1) The mass-balance variability of Outer Tropics glaciers in Bolivia is linked to 2 m air temperature ( $t$ ) and the El Niño-Southern Oscillation, (2) the glaciers of the Desert Andes are primarily influenced by zonal wind speed at 850 hPa and the Antarctic Oscillation

(AAO), (3) the glaciers of the Central Andes are mainly controlled by precipitation anomalies, dew-point temperature depression at 850 hPa ( $d_{pd}$ ) and the AAO, and (4) the mass-balance of the glacier Martial Este in the Fuegian Andes is linked to  $d_{pd}$  and summer  $t$ .

- The four distinct groups (above) are coincident with previously proposed classifications of South American glaciers. Our results therefore support the merits of the subdivision into the glaciological zones proposed by Lliboutry (1998) and updated by Barcaza and others (2017), and Zalazar and others (2020).
- The annual mass-balance EGMs have an average  $R^2$  value of  $\sim 0.45$  (0.15–0.74), and an average  $RMSE$  value of  $\sim 0.61$  m w.e (0.24–1.23 m w.e). The Outer Tropics EGMs perform worst ( $R^2 \approx 0.3$ ) and Desert Andes EGMs perform best ( $R^2 \approx 0.6$ ).
- The EGMs do not consider glacier dynamics or geometry, which are important factors for predicting the long-term mass-balance response to climate change. Therefore, they are currently only suitable for predicting short-term responses to perturbations in climate.
- The empirical relationship between Echaurren Norte's  $B_s$  and  $B_a$  breaks down from the 2000–2010 onward. This is likely related to the Central Chile Mega Drought.

The reader is advised to carefully consider the listed limitation and suggestions before applying this study's approach or results. While our results speak in favour of an EGM-based approach to glacier mass-balance modelling in South America, we suggest several measures to increase the accuracy and reliability of the models. A cross-validated LASSO approach may improve the EGMs, as its way to deal with multicollinearity may result in fewer problems than the approach used in this study. Furthermore, the glacier groups identified in this study may allow the pooling of data and the construction of more general, group-specific EGMs to circumvent the problem of the short mass-balance records. Another way to address this problem is by incorporating geodetic mass-balance records, and to use these to constrain mass-balance changes over specific observational periods and glaciological zones. Potential glacier regime shifts, i.e. non-stationary glacier-climate relationships, could also be addressed by a Bayesian model selection approach provided that observational records are long enough to allow the construction of regime-specific EGMs. Further improvement of the EGMs may be possible by considering topographic predictors in a deep-learning approach that would be able to capture important non-linear behaviour. Finally, we suggest the coupling of improved EGMs to a multi-model GCM ensemble to assess the effects of inter-model differences on mass-balance predictions.

**Supplementary material.** The supplementary material for this article can be found at <https://doi.org/10.1017/jog.2022.6>.

**Acknowledgements.** Support for this project was provided by DFG grant EH329/14-2 to T. Ehlers. We thank the European Centre for Medium Range Weather Forecasts for providing the ERA-Interim reanalysis data, and thank the World Glacier Monitoring Service (WGMS) for providing the glacier data used in this study. We also thank the World Climate Research Programme and the climate modelling groups, the Max Planck Institute for Meteorology, for producing and providing their model output. Finally, we thank the scientific editor Fanny Brun and the two anonymous reviewers for their very thorough and helpful reviews of our manuscript.

## References

Ayala A, Pellicciotti F, Peleg N and Burlando P (2017) Melt and surface sublimation across a glacier in a dry environment: distributed energy-balance modelling of Juncal Norte Glacier, Chile. *Journal of Glaciology* **63**(241), 803–822. doi: [10.1017/jog.2017.46](https://doi.org/10.1017/jog.2017.46)

- Barcaza G and 7 others (2017) Glacier inventory and recent glacier variations in the Andes of Chile, South America. *Annals of Glaciology* **58**(75pt2), 166–180. doi: [10.1017/aog.2017.28](https://doi.org/10.1017/aog.2017.28)
- Berrisford P and 9 others (2011) The ERA-Interim archive, version 2.0.
- Bolibar J and 5 others (2020) Deep learning applied to glacier evolution modelling. *The Cryosphere* **14**(2), 565–584. doi: [10.5194/tc-14-565-2020](https://doi.org/10.5194/tc-14-565-2020)
- Braithwaite RJ (2002) Glacier mass balance: the first 50 years of international monitoring. *Progress in Physical Geography* **26**(1), 76–95.
- Breiman L (2001) Random forests. *Machine learning* **45**(1), 5–32.
- Burger F and 7 others (2019) Interannual variability in glacier contribution to runoff from a high-elevation Andean catchment: understanding the role of debris cover in glacier hydrology. *Hydrological Processes* **33**(2), 214–229. doi: [10.1002/hyp.13354](https://doi.org/10.1002/hyp.13354)
- Buttstädt M, Möller M, Iturraspe R and Schneider C (2009) Mass balance evolution of Martial Este Glacier, Tierra del Fuego (Argentina) for the period 1960–2009. *Advances in Geosciences* **22**, 117–124. doi: [10.5194/adgeo-22-117-2009](https://doi.org/10.5194/adgeo-22-117-2009)
- Carrivick JL, Davies BJ, James WH, Quincey DJ and Glasser NF (2016) Distributed ice thickness and glacier volume in southern South America. *Global and Planetary Change* **146**, 122–132. doi: [10.1016/j.gloplacha.2016.09.010](https://doi.org/10.1016/j.gloplacha.2016.09.010)
- Cavazos T and Hewitson BC (2005) Performance of NCEP–NCAR reanalysis variables in statistical downscaling of daily precipitation. *Climate Research* **28**(2), 95–107. doi: [10.3354/cr028095](https://doi.org/10.3354/cr028095)
- Charles S, Bates B, Whetton P and Hughes J (1999) Validation of downscaling models for changed climate conditions: case study of southwestern Australia. *Climate Research* **12**, 1–14. doi: [10.3354/cr012001](https://doi.org/10.3354/cr012001)
- Cogley JG and 9 others (2011) Glossary of glacier mass balance and related terms. *IHP-VII technical documents in hydrology* **86**, 965.
- Condom T, Coudrain A, Sicart JE and Théry S (2007) Computation of the space and time evolution of equilibrium-line altitudes on Andean glaciers (10°N–55°S). *Global and Planetary Change* **59**(1), 189–202. doi: [10.1016/j.gloplacha.2006.11.021](https://doi.org/10.1016/j.gloplacha.2006.11.021)
- Cuffey KM and Paterson WSB (2010) *The Physics of Glaciers*. Academic Press. ISBN 978-0-08-091912-6.
- Dee DP and 35 others (2011) The ERA-Interim reanalysis: configuration and performance of the data assimilation system. *Quarterly Journal of the Royal Meteorological Society* **137**(656), 553–597.
- Douglas BC, Kearney MS, Leatherman SP (2001) *Sea level rise: history and consequences*, Volume 75 of *International Geophysics Series*. Academic Press, San Diego.
- Egholm DL, Nielsen SB, Pedersen VK and Lesemann JE (2009) Glacial effects limiting mountain height. *Nature* **460**(7257), 884–887. doi: [10.1038/nature08263](https://doi.org/10.1038/nature08263)
- Farinotti D and 6 others (2019) A consensus estimate for the ice thickness distribution of all glaciers on earth. *Nature Geoscience* **12**, 168–173. doi: [10.1038/s41561-019-0300-3](https://doi.org/10.1038/s41561-019-0300-3)
- Favier V, Falvey M, Rabatel A, Praderio E and López D (2009) Interpreting discrepancies between discharge and precipitation in high-altitude area of Chile's Norte Chico region (26–32°S). *Water Resources Research* **45**(2), W02424. doi: [10.1029/2008WR006802](https://doi.org/10.1029/2008WR006802)
- Fernández A and Mark BG (2016) Modeling modern glacier response to climate changes along the Andes Cordillera: a multiscale review. *Journal of Advances in Modeling Earth Systems* **8**(1), 467–495. doi: [10.1002/2015MS000482](https://doi.org/10.1002/2015MS000482)
- Francou B, Ribstein P, Saravia R and Tiriau E (1995) Monthly balance and water discharge of an inter-tropical glacier: Zongo Glacier, Cordillera Real, Bolivia, 16 S. *Journal of Glaciology* **41**(137), 61–67.
- Francou B, Vuille M, Favier V and Cáceres B (2004) New evidence for an ENSO impact on low-latitude glaciers: Antizana 15, Andes of Ecuador, 0° 28'S. *Journal of Geophysical Research: Atmospheres* **109**(D18), D18106. doi: [10.1029/2003JD004484](https://doi.org/10.1029/2003JD004484)
- Gao L, Schulz K and Bernhardt M (2014) Statistical downscaling of ERA-Interim forecast precipitation data in complex terrain Using LASSO algorithm. *Advances in Meteorology* **2014**, 472741.
- Garreaud R, Lopez P, Minvielle M and Rojas M (2013) Large-scale control on the Patagonian climate. *Journal of Climate* **26**(1), 215–230. doi: [10.1175/JCLI-D-12-00001.1](https://doi.org/10.1175/JCLI-D-12-00001.1)
- Garreaud RD, Vuille M, Compagnucci R and Marengo J (2009) Present-day South American climate. *Palaeogeography, Palaeoclimatology, Palaeoecology* **281**(3), 180–195. doi: [10.1016/j.palaeo.2007.10.032](https://doi.org/10.1016/j.palaeo.2007.10.032)
- Garreaud RD and 5 others (2019) The central Chile mega drought (2010–2018): a climate dynamics perspective. *International Journal of Climatology* **40**(1), 421–439. doi: [10.1002/joc.6219](https://doi.org/10.1002/joc.6219)

- Gillett NP, Kell TD and Jones PD (2006) Regional climate impacts of the Southern Annular Mode. *Geophysical Research Letters* **33**(23), L23704. doi: [10.1029/2006GL027721](https://doi.org/10.1029/2006GL027721).
- Giorgi F and 9 others (2011) Regional climate information – evaluation and projections. In *Climate Change 2001: The Scientific Basis*, 583–638, Cambridge University Press, Cambridge.
- Gurgiser W, Marzeion B, Ortner M and Kaser G (2014) Modeling mass balance of a tropical glacier in the Peruvian Andes. In *EGU General Assembly Conference Abstracts*, Vol. 16, 3798.
- Hammami D, Lee TS, Ouarda TB and Lee J (2012) Predictor selection for downscaling GCM data with LASSO. *Journal of Geophysical Research: Atmospheres* **117**(D17), D17116.
- Ho M, Kiem AS and Verdon-Kidd DC (2012) The Southern Annular Mode: a comparison of indices. *Hydrology and Earth System Sciences* **16**(3), 967–982. doi: [10.5194/hess-16-967-2012](https://doi.org/10.5194/hess-16-967-2012)
- Hodge SM and 5 others (1998) Climate variations and changes in mass of three glaciers in Western North America. *Journal of Climate* **11**(9), 2161–2179. doi: [10.1175/1520-0442\(1998\)011<2161:CVACIM>2.0.CO;2](https://doi.org/10.1175/1520-0442(1998)011<2161:CVACIM>2.0.CO;2)
- Hoinkes HC (1968) Glacier variation and weather. *Journal of Glaciology* **7**(49), 3–18.
- Hostetler SW and Clark PU (2000) Tropical climate at the last glacial maximum inferred from glacier mass-balance modeling. *Science* **290**(5497), 1747–1750. doi: [10.1126/science.290.5497.1747](https://doi.org/10.1126/science.290.5497.1747)
- Hulton NRJ, Purves RS, McCulloch RD, Sugden DE and Bentley MJ (2002) The last glacial maximum and deglaciation in southern South America. *Quaternary Science Reviews* **21**(1), 233–241. doi: [10.1016/S0277-3791\(01\)00103-2](https://doi.org/10.1016/S0277-3791(01)00103-2)
- Huss M and Hock R (2018) Global-scale hydrological response to future glacier mass loss. *Nature Climate Change* **8**(2), 135–140. doi: [10.1038/s41558-017-0049-x](https://doi.org/10.1038/s41558-017-0049-x)
- Huth R (2002) Statistical downscaling of daily temperature in Central Europe. *Journal of Climate* **15**(13), 1731–1742. doi: [10.1175/1520-0442\(2002\)015<1731:SDODTI>2.0.CO;2](https://doi.org/10.1175/1520-0442(2002)015<1731:SDODTI>2.0.CO;2)
- IPCC (2021) *IPCC, 2021: Climate Change 2021: The Physical Science Basis. Contribution of Working Group I to the Sixth Assessment Report of the Intergovernmental Panel on Climate Change*. Cambridge University Press.
- Jóhannesson T, Raymond C and Waddington E (1989) Time-scale for adjustment of glaciers to changes in mass balance. *Journal of Glaciology* **35**(121), 355–369. doi: [10.3189/S002214300000928X](https://doi.org/10.3189/S002214300000928X)
- Kaser G, Juen I, Georges C, Gómez J and Tamayo W (2003) The impact of glaciers on the runoff and the reconstruction of mass balance history from hydrological data in the tropical Cordillera Blanca, Perú. *Journal of Hydrology* **282**(1), 130–144. doi: [10.1016/S0022-1694\(03\)00259-2](https://doi.org/10.1016/S0022-1694(03)00259-2)
- Kaser G, Cogley JG, Dyurgerov MB, Meier MF and Ohmura A (2006) Mass balance of glaciers and ice caps: consensus estimates for 1961–2004. *Geophysical Research Letters* **33**(19), L19501. doi: [10.1029/2006GL027511](https://doi.org/10.1029/2006GL027511).
- Kaser G, Großhauser M and Marzeion B (2010) Contribution potential of glaciers to water availability in different climate regimes. *Proceedings of the National Academy of Sciences* **107**(47), 20223–20227. doi: [10.1073/pnas.1008162107](https://doi.org/10.1073/pnas.1008162107)
- Kull C, Hänni F, Grosjean M and Veit H (2003) Evidence of an LGM cooling in NW-Argentina (22°S) derived from a glacier climate model. *Quaternary International* **108**(1), 3–11. doi: [10.1016/S1040-6182\(02\)00190-8](https://doi.org/10.1016/S1040-6182(02)00190-8)
- Leatherman SP (2001) Social and economic costs of sea level rise. In BC Douglas, MS Kearney and SP Leatherman (eds.), *Sea Level Rise*, volume 75 of *International Geophysics Series*, 181–223, Academic Press, San Diego.
- Liboutry L (1974) Multivariate statistical analysis of glacier annual balances. *Journal of Glaciology* **13**(69), 371–392. doi: [10.3189/S0022143000023169](https://doi.org/10.3189/S0022143000023169)
- Liboutry L (1998) Glaciers of South America. In RS Williams and JG Ferrigno (eds.), *Satellite image atlas of glaciers of the world*, US Geological Survey.
- MacDonell S, Kinnard C, Mölg T, Nicholson L and Abermann J (2013) Meteorological drivers of ablation processes on a cold glacier in the semi-arid Andes of Chile. *The Cryosphere* **7**(5), 1513–1526. doi: [10.5194/tc-7-1513-2013](https://doi.org/10.5194/tc-7-1513-2013)
- Magalhães N and Evangelista H (2018) Wildfires in South America and its impact on the central Andes glaciers. In *EGU General Assembly Conference Abstracts*, volume 20, 10986.
- Manciati C and 5 others (2014) Empirical mass balance modelling of South American tropical glaciers: case study of Antisana volcano, Ecuador. *Hydrological Sciences Journal* **59**(8), 1519–1535. doi: [10.1080/02626667.2014.888490](https://doi.org/10.1080/02626667.2014.888490)
- Marengo JA, Soares WR, Saulo AC and Nicolini M (2004) Climatology of the low-level jet east of the Andes as derived from the NCEP–NCAR reanalyses: characteristics and temporal variability. *Journal of Climate* **17**, 2261–2280. doi: [10.1175/1520-0442\(2004\)017<2261:COTLJE>2.0.CO;2](https://doi.org/10.1175/1520-0442(2004)017<2261:COTLJE>2.0.CO;2)
- Marzeion B, Hofer M, Jarosch AH, Kaser G and Mölg T (2012) A minimal model for reconstructing interannual mass balance variability of glaciers in the European Alps. *The Cryosphere* **6**(1), 71–84. doi: [10.5194/tc-6-71-2012](https://doi.org/10.5194/tc-6-71-2012)
- Masiokas MH and 9 others (2016) Reconstructing the annual mass balance of the Echaurren Norte glacier (Central Andes, 33.5° S) using local and regional hydroclimatic data. *The Cryosphere* **10**(2), 927–940.
- Maussion F, Gurgiser W, Großhauser M, Kaser G and Marzeion B (2015) ENSO influence on surface energy and mass balance at Shallap Glacier, Cordillera Blanca, Peru. *The Cryosphere* **9**(4), 1663–1683. doi: [10.5194/tc-9-1663-2015](https://doi.org/10.5194/tc-9-1663-2015)
- Maussion F and 15 others (2019) The Open Global Glacier Model (OGGM) v1.1. *Geoscientific Model Development* **12**(3), 909–931. doi: [10.5194/gmd-12-909-2019](https://doi.org/10.5194/gmd-12-909-2019)
- Meier MF (1984) Contribution of small glaciers to global sea level. *Science* **226**(4681), 1418–1421. doi: [10.1126/science.226.4681.1418](https://doi.org/10.1126/science.226.4681.1418)
- Mernild SH and 6 others (2015) Mass loss and imbalance of glaciers along the Andes Cordillera to the sub-Antarctic islands. *Global and Planetary Change* **133**, 109–119. doi: [10.1016/j.gloplacha.2015.08.009](https://doi.org/10.1016/j.gloplacha.2015.08.009)
- Mernild SH, Liston GE, Hiemstra C and Wilson R (2017) The Andes Cordillera. Part III: Glacier surface mass balance and contribution to sea level rise (1979–2014). *International Journal of Climatology* **37**(7), 3154–3174. doi: [10.1002/joc.4907](https://doi.org/10.1002/joc.4907)
- Michaelsen J (1987) Cross-validation in statistical climate forecast models. *Journal of Climate and Applied Meteorology* **26**(11), 1589–1600. doi: [10.1175/1520-0450\(1987\)026<1589:CVISCF>2.0.CO;2](https://doi.org/10.1175/1520-0450(1987)026<1589:CVISCF>2.0.CO;2)
- Mölg T and Kaser G (2011) A new approach to resolving climate-cryosphere relations: downscaling climate dynamics to glacier-scale mass and energy balance without statistical scale linking. *Journal of Geophysical Research: Atmospheres* **116**(D16), D16101. doi: [10.1029/2011JD015669](https://doi.org/10.1029/2011JD015669).
- Molina LT and 17 others (2015) Pollution and its impacts on the South American cryosphere. *Earth's Future* **3**(12), 345–369. doi: [10.1002/2015EF000311](https://doi.org/10.1002/2015EF000311)
- Müller P (1987) *Parametrisierung der Gletscher-Klima-Beziehung für die Praxis: Grundlagen und Beispiele*. Doctoral Thesis, ETH Zurich (doi: [10.3929/ethz-a-000472787](https://doi.org/10.3929/ethz-a-000472787)).
- Mutz S, Paeth H and Winkler S (2015) Modelling of future mass balance changes of Norwegian glaciers by application of a dynamical–statistical model. *Climate Dynamics* **46**(5), 1581–1597. doi: [10.1007/s00382-015-2663-5](https://doi.org/10.1007/s00382-015-2663-5)
- Mutz SG and Ehlers TA (2019) Detection and explanation of spatiotemporal patterns in late cenozoic palaeoclimate change relevant to earth surface processes. *Earth Surface Dynamics* **7**(3), 663–679. doi: [10.5194/esurf-7-663-2019](https://doi.org/10.5194/esurf-7-663-2019)
- Mutz SG, Scherrer S, Muceniece I and Ehlers TA (2021) Twenty-first century regional temperature response in Chile based on empirical–statistical downscaling. *Climate Dynamics* **56**(18), 1432–0894. doi: [10.1007/s00382-020-05620-9](https://doi.org/10.1007/s00382-020-05620-9)
- NOAA (2005) Climate Prediction Center: teleconnection pattern calculation procedures. [https://www.cpc.ncep.noaa.gov/products/precip/CWlink/daily\\_ao\\_index/history/method.shtml](https://www.cpc.ncep.noaa.gov/products/precip/CWlink/daily_ao_index/history/method.shtml).
- Oerlemans J (1992) Climate sensitivity of glaciers in southern Norway: application of an energy-balance model to Nigardsbreen, Hellstugubreen and Alftobreen. *Journal of Glaciology* **38**(129), 223–232. doi: [10.3189/S0022143000003634](https://doi.org/10.3189/S0022143000003634)
- Oerlemans J (1993) Modelling of glacier mass balance. In WR Peltier (ed.), *Ice in the Climate System*, Vol. 12 in NATO ASI Series, 101–116, Springer Berlin Heidelberg.
- Oerlemans J and Reichert BK (2000) Relating glacier mass balance to meteorological data by using a seasonal sensitivity characteristic. *Journal of Glaciology* **46**(152), 1–6. doi: [10.3189/172756500781833269](https://doi.org/10.3189/172756500781833269)
- Pellicciotti F and 7 others (2008) A study of the energy balance and melt regime on Juncal Norte Glacier, semi-arid Andes of central Chile, using melt models of different complexity. *Hydrological Processes* **22**(19), 3980–3997. doi: [10.1002/hyp.7085](https://doi.org/10.1002/hyp.7085)
- Pfeffer WT and 19 others (2014) The Randolph Glacier Inventory: a globally complete inventory of glaciers. *Journal of Glaciology* **60**(221), 537–552. doi: [10.3189/2014JG13J176](https://doi.org/10.3189/2014JG13J176)
- Quintana JM and Aceituno P (2012) Changes in the rainfall regime along the extratropical west coast of South America (Chile): 30–43° S. *Atmósfera* **25**(1), 1–22.

- Rabatel A, Castebrunet H, Favier V, Nicholson L and Kinnard C (2011) Glacier changes in the Pascua-Lama region, Chilean Andes (29° S): recent mass balance and 50 yr surface area variations. *The Cryosphere* 5(4), 1029–1041. doi: [10.5194/tc-5-1029-2011](https://doi.org/10.5194/tc-5-1029-2011)
- Rabatel A and 27 others (2013) Current state of glaciers in the tropical Andes: a multi-century perspective on glacier evolution and climate change. *The Cryosphere* 7(1), 81–102. doi: [10.5194/tc-7-81-2013](https://doi.org/10.5194/tc-7-81-2013)
- Ragetti S, Immerzeel WW and Pellicciotti F (2016) Contrasting climate change impact on river flows from high-altitude catchments in the Himalayan and Andes Mountains. *Proceedings of the National Academy of Sciences* 113(33), 9222–9227. doi: [10.1073/pnas.1606526113](https://doi.org/10.1073/pnas.1606526113)
- Reichert BK, Bengtsson L and Oerlemans J (2001) Midlatitude forcing mechanisms for glacier mass balance investigated using general circulation models. *Journal of Climate* 14(17), 3767–3784. doi: [10.1175/1520-0442\(2001\)014<3767:MFMFGM>2.0.CO;2](https://doi.org/10.1175/1520-0442(2001)014<3767:MFMFGM>2.0.CO;2)
- Rhoades RE, Ríos XZ and Aragundy J (2006) Climate change in Cotacachi. In RE Rhoades (ed.), *Development with Identity: Community, Culture and Sustainability in the Andes*, 64–74, CABI Publishing, Wallingford, UK.
- Ribstein P, Tiriau E, Francou B and Saravia R (1995) Tropical climate and glacier hydrology: a case study in Bolivia. *Journal of Hydrology* 165(1), 221–234. doi: [10.1016/0022-1694\(94\)02572-S](https://doi.org/10.1016/0022-1694(94)02572-S)
- Sagredo E and Lowell T (2012) Climatology of Andean glaciers: a framework to understand glacier response to climate change. *Global and Planetary Change* 86–87, 101–109. doi: [10.1016/j.gloplacha.2012.02.010](https://doi.org/10.1016/j.gloplacha.2012.02.010)
- Sagredo EA, Rupper S and Lowell TV (2014) Sensitivities of the equilibrium line altitude to temperature and precipitation changes along the Andes. *Quaternary Research* 81(2), 355–366. doi: [10.1016/j.yqres.2014.01.008](https://doi.org/10.1016/j.yqres.2014.01.008)
- Sagredo EA and 6 others (2017) Equilibrium line altitudes along the Andes during the last millennium: paleoclimatic implications. *The Holocene* 27(7), 1019–1033. doi: [10.1177/0959683616678458](https://doi.org/10.1177/0959683616678458)
- Schaefer M, Machguth H, Falvey M and Casassa G (2013) Modeling past and future surface mass balance of the Northern Patagonia Icefield. *Journal of Geophysical Research: Earth Surface* 118(2), 571–588. doi: [10.1002/jgrf.20038](https://doi.org/10.1002/jgrf.20038)
- Schöner W and Böhm R (2007) A statistical mass-balance model for reconstruction of LIA ice mass for glaciers in the European Alps. *Annals of Glaciology* 46, 161–169. doi: [10.3189/172756407782871639](https://doi.org/10.3189/172756407782871639)
- Shiklomanov I (1993) World fresh water resources. In PH Gleick (ed.), *Water in Crisis*, Oxford University Press, New York, NY.
- Sicart JE, Ribstein P, Francou B, Pouyaud B and Condom T (2007) Glacier mass balance of tropical Zongo glacier, Bolivia, comparing hydrological and glaciological methods. *Global and Planetary Change* 59(1), 27–36. doi: [10.1016/j.gloplacha.2006.11.024](https://doi.org/10.1016/j.gloplacha.2006.11.024)
- Silvestri GE and Vera CS (2003) Antarctic Oscillation signal on precipitation anomalies over southeastern South America. *Geophysical Research Letters* 30(21), 2115. doi: [10.1029/2003GL018277](https://doi.org/10.1029/2003GL018277)
- Stocker TF and 9 others (2013) *Climate Change 2013: the physical science basis: contribution of Working Group I to the Fifth Assessment Report of the Intergovernmental Panel on Climate Change*. Intergovernmental Panel on Climate Change, Cambridge.
- Strelin J and Iturraspe R (2007) Recent evolution and mass balance of Cordón Martial glaciers, Cordillera Fuegoina Oriental. *Global and Planetary Change* 59(1–4), 17–26. doi: [10.1016/j.gloplacha.2006.11.019](https://doi.org/10.1016/j.gloplacha.2006.11.019)
- Tangborn W (1999) A mass balance model that uses low-altitude meteorological observations and the area–altitude distribution of a glacier. *Geografiska Annaler: Series A, Physical Geography* 81(4), 753–765. doi: [10.1111/1468-0459.00103](https://doi.org/10.1111/1468-0459.00103)
- Thomson SN and 5 others (2010) Glaciation as a destructive and constructive control on mountain building. *Nature* 467(7313), 313–317. doi: [10.1038/nature09365](https://doi.org/10.1038/nature09365)
- Tibshirani R (1996) Regression shrinkage and selection via the Lasso. *Journal of the Royal Statistical Society: Series B (Methodological)* 58(1), 267–288. doi: [10.1111/j.2517-6161.1996.tb02080.x](https://doi.org/10.1111/j.2517-6161.1996.tb02080.x)
- Veettil BK, Bremer UF, de Souza SF, ÉLB M. and Simões JC (2016) Influence of ENSO and PDO on mountain glaciers in the outer tropics: case studies in Bolivia. *Theoretical and Applied Climatology* 125(3), 757–768. doi: [10.1007/s00704-015-1545-4](https://doi.org/10.1007/s00704-015-1545-4)
- Vergara W and 7 others (2007) Economic impacts of rapid glacier retreat in the Andes. *Eos, Transactions American Geophysical Union* 88(25), 261–264. doi: [10.1029/2007EO250001](https://doi.org/10.1029/2007EO250001)
- Von Storch H and Zwiers FW (2003) *Statistical Analysis in Climate Research*. 1. paperback ed., Cambridge Univ. Press, Cambridge. reprinted. edition.
- Vuille M and Milana JP (2007) High-latitude forcing of regional aridification along the subtropical west coast of South America. *Geophysical Research Letters* 34(23), L23703. doi: [10.1029/2007GL031899](https://doi.org/10.1029/2007GL031899)
- Wagnon P, Ribstein P, Francou B and Sicart JE (2001) Anomalous heat and mass budget of Glaciar Zongo, Bolivia, during the 1997/98 El Niño year. *Journal of Glaciology* 47(156), 21–28.
- WGMS (2017) *Global Glacier Change Bulletin No. 2 (2014–2015)*. World Glacier Monitoring Service, Zurich, Switzerland.
- WGMS (2018) *Fluctuations of glaciers database*. World Glacier Monitoring Service, Zurich, Switzerland.
- Wilby R and 5 others (2004) Guidelines for use of climate scenarios developed from statistical downscaling methods. *Supporting material of the Intergovernmental Panel on Climate Change, available from the DDC of IPCC TG CIA*, 27.
- Wilks DS (2006) *Statistical methods in the atmospheric sciences*. Vol. 91 in International Geophysics Series, Academic Press, Amsterdam; Boston, 2nd ed edition, ISBN 978-0-12-751966-1.
- Winkler S and Nesje A (2009) Perturbation of climatic response at maritime glaciers?. *Erdkunde* 63(3), 229–244. doi: [10.3112/erdkunde.2009.0](https://doi.org/10.3112/erdkunde.2009.0)
- Wolter K and Timlin MS (1993) Measuring ENSO and COADS with a seasonally adjusted principal component index. In *Proceedings of the 17th Climate Diagnostics Workshop*, 1993.
- Wolter K and Timlin MS (2011) El Niño/Southern oscillation behaviour since 1871 as diagnosed in an extended multivariate ENSO index (MEI.ext). *International Journal of Climatology* 31(7), 1074–1087. doi: [10.1002/joc.2336](https://doi.org/10.1002/joc.2336)
- Zalazar L and 9 others (2020) Spatial distribution and characteristics of andean ice masses in argentina: results from the first national glacier inventory. *Journal of Glaciology* 66(260), 938–949. doi: [10.1017/jog.2020.55](https://doi.org/10.1017/jog.2020.55)
- Zekollari H, Huss M and Farinotti D (2020) On the imbalance and response time of glaciers in the European Alps. *Geophysical Research Letters* 47(2), e2019GL085578. doi: [10.1029/2019GL085578](https://doi.org/10.1029/2019GL085578)
- Zemp M and 14 others (2019) Global glacier mass changes and their contributions to sea-level rise from 1961 to 2016. *Nature* 568, 382–386. doi: [10.1038/s41586-019-1071-0](https://doi.org/10.1038/s41586-019-1071-0)
- Zhang P (1993) Model selection via multifold cross validation. *The Annals of Statistics* 21(1), 299–313. doi: [10.1214/aos/1176349027](https://doi.org/10.1214/aos/1176349027)
- Zolles T, Maussion F, Galos SP, Gurgiser W and Nicholson L (2019) Robust uncertainty assessment of the spatio-temporal transferability of glacier mass and energy balance models. *The Cryosphere* 13(2), 469–489. doi: [10.5194/tc-13-469-2019](https://doi.org/10.5194/tc-13-469-2019)